A STUDY OF DISPERSIVE BEHAVIOUR IN MICROSTRIP TRANSMISSION LINES

BY

O. P. JAIN

CARLETON UNIVERSITY

FACULTY OF ENGINEERING

TECHNICAL REPORT

MAY 1971

A STUDY OF DISPERSIVE BEHAVIOUR IN MICROSTRIP TRANSMISSION LINES

by

O.P. Jain, M.Sc. (Tech)

This report is prepared for the Communication Research Centre, Department of Communication under contract, Serial No. OGRO-151.

Division of Electronics and Materials Engineering

Carleton University

Ottawa, Ontario,

May, 1971.

ACKNOWLEDGEMENTS

The author is indebted to his thesis supervisor Dr. V. Makios for his support and encouragement during the course of this work reported here, and particularly for helpful discussions. The author wishes to express his deep appreciation to Dr. W.J. Chudobiak of Communications Research Centre, Ottawa, for introducing him to the field of Microwave Integrated Circuits, for his encouragement, and especially for numerous useful suggestions during the course of this work.

The author is grateful to Roman Radzichowsky and Earl Doherty of Communications Research Centre workshop in their assistance in the fabrication of experimental microstrip structures.

The financial support provided by the Dept. of Communications (OGRO-151) and the National Research Council of Canada (Grant No. 4730) is gratefully acknowledged.

Finally the author wishes to thank Miss Carol Delorme for her patience and effort in typing this manuscript.

ABSTRACT

The apparent variation of the effective dielectric constant of microstrip transmission lines with frequency is studied experimentally, empirically and analytically. The experimental techniques for the measurement of dispersion are described. Empirical relations are derived from the experimental results which describe (with in an accuracy of $\pm$ 5%) the dispersive behaviour in microstrip transmission lines for a wide range of dielectric constants ($2 \leq \varepsilon_r \leq 10$), substrate thickness (0.020 inch $\leq h \leq$ 0.125 inch) and $\frac{w}{h}$ ratios ($0.9 \leq \frac{w}{h} \leq 13$).

A coupled mode analysis of dispersion in microstrip transmission lines is developed by considering the coupling between the TEM mode and the TM_o surface wave mode. An expression for the coupling coefficient is derived from a series of qualitative arguments and experimental results on dispersion. The analysis accounts for dispersion (within an accuracy of $\pm$ 2%) in microstrip transmission lines for a wide range of microstrip line parameters ($2 \leq \varepsilon_r \leq 104$; .020 inch $\leq h \leq$ 0.125 inch; $0.9 \leq \frac{w}{h} \leq 6$).

TABLE OF CONTENTS

TABLE OF CONTENTS (Cont'd)

LIST OF FIGURES

LIST OF FIGURES (Cont'd)

LIST OF FIGURES (Cont'd)

LIST OF SYMBOLS

a	Mode Amplitude of the Propagating Wave
a_i	Amplitude of the i^{th} mode of Propagation
β	Propagation Constant of the Propagating Wave on a Microstrip Line
β_a	Free space wave number
β_{co}	Cut off propagation constant of the surface waves
β_{rr}	Uncoupled propagation constant of the rth mode
β_{rs}	Coupling Coefficient between the rth and sth mode (in same units as β)
β_o	Propagation constant of the TEM mode Microstrip line mode
β_{TM}	Propagation constant of the TM surface wave mode
β_{TM_o}	Propagation constant of the lowest order TM surface wave mode
BW	Half power bandwidth
C	Velocity of light
CRO	Cathode ray oscilloscope
D_{mean}	Mean diameter of the resonant ring
Δf_{mr}	Half power bandwidth
$\bar{E}$	Electric Field vector
ε	Permitivity of the substrate material
ε_o	Permitivity of the free space
ε_r	Relative permitivity or Relative dielectric constant of the substrate material
ε_{eff}	Effective dielectric constant of the propagating wave on the microstrip line
ε_{eff_o}	Effective dielectric constant of the TEM mode

$\varepsilon_{eff_{TM_o}}$	Effective dielectric constant of the TM_o surface wave mode
$\varepsilon_{12}=\varepsilon_{21}$	Passive coupling coefficient between the quasi-TEM microstrip line mode and the TM_o wave mode
f	Frequency
f_ℓ	Upper frequency limit on the operation of the microstrip transmission lines
f_{ℓ_n}	Upper frequency limit for narrow microstrip lines
f_{mr}	Resonant frequency of the transmission cavity
f_o	Frequency in Giga-Hertz below which dispersion is negligible
f'	$(f-f_o)$ in GHz
h	Thickness of the substrate material of the microstrip line
$\overline{H}$	Magnetic field vector
i	Current
j	$(-1)^{\frac{1}{2}}$
ℓ	Length
λ	Wavelength of the electromagnetic wave
λ_c	Wavelength of the propagating wave in the coaxial line
λ_m	Wavelength of the propagating wave on the microstrip transmission line
λ_{mr}	Wavelength of the propagating wave on the microstrip transmission line resonator at resonance
λ_a	Wavelength of the electromagnetic wave in free space
λ_d	Wavelength of the electromagnetic wave in the dielectric medium
mil	10^{-3} inch
ω	Angular frequency in radians

p_a	Transverse wave number of the TM_o surface wave in the air
p_d	Transverse wave number of the TM_o surface wave in the dielectric
P_{rad}	Power radiated from the microstrip
Q	Quality factor
Q_L	Loaded quality factor
Q_o	Unloaded quality factor
Q_{ext}	External quality factor
Q_{rad}	Radiation quality factor
R	Inner radius of the resonant ring cavity
t	Thickness of the strip conductor of the microstrip line
TE	Transverse Electric
TM	Transverse Magnetic
TEM	Transverse Electromagnetic
v	Voltage
v_{ph}	Phase Velocity
w	Width of the strip conductor of the microstrip line
w'	Effective width of the strip conductor of the microstrip line[14]

$$w + \frac{t}{\pi}\left(1 + \ell n \frac{4\pi w}{t}\right) \text{ for } \frac{w}{h} \leq \frac{1}{2\pi}$$

$$w + \frac{t}{\pi}\left(1 + \ell n \frac{2h}{t}\right) \text{ for } \frac{w}{h} \geq \frac{1}{2\pi}$$

y_o	Characteristic admittance of the propagating wave on the microstrip line
y_{oo}	Characteristic admittance of the TEM Mode
Z_o	Characteristic impedance of the propagating wave on the microstrip line
Z_{oo}	Characteristic impedance of the TEM Mode

CHAPTER 1

INTRODUCTION

1.1 Introduction

The advent of microwave semiconductor devices has stimulated interest in microwave integrated circuits and hence in microstrip transmission lines and circuit elements. Various workers[1-8] have reported on the frequency dependence of the phase velocity (or the effective dielectric constant) of the propagating mode in microstrip transmission lines. Experimental results, reported to date, show that the dispersive effects are quite significant above about 2 GHz, particularly for thick ($h > 50$ mils) and high dielectric constant ($\varepsilon_r > 10$) substrates. However, the existing literature does not give adequate qualitative and quantitative analysis of dispersion in microstrip transmission lines. Consequently, the study of dispersion in microstrip transmission lines is the subject of this thesis.

1.2 Characteristics and Limitations of Microstrip Transmission Lines

A planar transmission line consisting of a strip conductor spaced from a ground plane by a dielectric layer is known as a microstrip transmission line[9]. The schematic diagram of a microstrip transmission line, shown in figure 1, defines the dimensional parameters of the structure. A conducting ground plane (of nominally

infinite extent) supports a uniform layer of dielectric material of thickness h, upon which is located a thin conducting strip of width w and thickness t.

Microstrip circuit elements offer the following advantages over strip line, coaxial and waveguide elements:[10]

i) The complete conductor pattern may be deposited and processed on a single dielectric substrate which is supported by a single metal ground plane. Such a circuit may be fabricated at a substantially lower cost than strip line, waveguide or coaxial circuit configurations.

ii) Both packaged and unpackaged semiconductor chips may be conveniently attached to the microstrip element because of the planar nature of the structure.

iii) Devices and components incorporated into hybrid microwave integrated circuits are accessible for probing and measurement purposes.

However, microstrip transmission lines suffer from the following limitations:

i) Microstrip transmission lines have higher radiation losses than strip line, coaxial or waveguide structures. The radiation losses have been theoretically calculated by Lewin[11] and experimentally verified by Denlinger[12].

Denlinger's results are reproduced in figures 3 and 4. One observes from these results that the radiation losses from microstrip transmission lines are strongly dependent on the thickness and the dielectric constant of the substrate material. These results also show that the radiation losses may be reduced by choosing thin substrates with high dielectric constants.

ii) Proximity of the air-dielectric air interface with the strip conductor causes a discontinuity in the electric and the magnetic fields (see figure 2) at the interface.[13] In fact, there are components of both electric and magnetic fields in the direction of propagation. The propagation mode, therefore, is not a pure TEM Mode *(a mode in which both the electric and magnetic fields are normal to the direction of the wave propagation, a condition for which approximate solutions may be obtained using electrostatic approximations)*[14,15,16]. However, at low frequencies, ($h < \lambda_d/30$) the actual propagating mode (commonly referred to as quasi-TEM mode) closely resembles a TEM mode and therefore the various electrostatic approximations such as 'conformal mapping'[14], relaxation method [15] and variational principle[16] may be used. Wheeler's[14] quasi-static solution, based on conformal mapping is suitable for calculating the

characteristic impedance, the phase velocity and the wavelength of a single microstrip transmission line at low frequencies.[17]

In 1957, Wu[18] reported a theoretical analysis of the electric and magnetic fields in microstrip transmission lines. He established coupled integral equations for the current densities I_x and I_z on the strip conductor (see figure 1 for coordinates), which he suggested could be solved by numerical methods. Later Delogne[19] pointed out that the path of integration chosen by Wu leads to growing waves perpendicular to the strip and so is in error. However, even if it is possible to find a suitable path of integration the approach seems to be complex and may require extensive, rigorous and lengthy numerical computations to get any results, and so this approach has not been considered in this thesis.

However, at high frequencies ($h > \lambda_d/30$), the dispersion of the non-TEM modes causes a considerable deviation in the effective dielectric constant and the velocity of propagation predicted by the electrostatic approximation. A literature survey on the dispersive behaviour of microstrip transmission lines is given in the following section.

1.3 Literature Survey of Dispersion in Microstrip Transmission Lines

In 1968, Hartwig et al[1] reported measurements of the effective dielectric constant of the propagating mode in microstrip transmission

lines on rutile and alumina substrates (see figures 5 and 6). To explain this behaviour, they proposed a theory based on synchronous coupling of the TEM mode and a TM_o surface wave mode (*the surface waves exist due to the air dielectric interface, the TM_o being the dominant mode of propagation*).[20] However, a theoretical derivation of the coupling coefficient of the two modes was not given, since they lacked an explicit description of the electric and magnetic fields. Instead empirically derived expressions for the coupling coefficients were described to fit the experimental data (see figures 5 and 6). However, such empirical relations are of limited practical use since they cannot be used to calculate the dispersion for any other mateiral or even for the same material with different $\frac{w}{h}$ and h parameters.

In January 1969, Troughton[2,3] reported a new technique for measuring dispersion in microstrip transmission lines. He measured the wavelength of the propagating mode on microstrip transmission lines by using a microstrip transmission line ring structure (figure 7) and noting the frequencies at which the ring resonated. Resonance occurs whenever the mean circumference of the ring equals an integer multiple of a wavelength at that frequency. As is described in Chapter 2, this technique gives more accurate results compared to earlier methods using open or short circuit terminations. In the same paper, Troughton presented dispersion measurement results for microstrip transmission lines on an alumina substrate (see figure 8). No theory was given or suggested to explain the dispersive behaviour of microstrip transmission lines.

In May 1969, Zysman and Varon[4] reported that the modes that exist on the microstrip transmission lines are a linear combination of TE and TM modes. In this analysis, TE and TM modes each satisfy the wave equations and boundary conditions with the exception of the boundary at the strip conductor; their linear combination satisfying the boundary conditions at the strip conductor. The final result of the analysis of a microstrip transmission line enclosed in a large metallic box* is a pair of coupled integral equations which were solved numerically. Their theoretical results were in close agreement with their measured results on a 50 ohm microstrip transmission line ($\varepsilon_r = 9.7$, h = 50 mils, $\frac{w}{h} = 1$) in the frequency range of 1 to 10GHz. However, the analysis requires lengthy computer computations and is not convenient for microstrip component design.

In June 1969, Napoli and Hughes[5] reported experimental results on the dispersive behaviour of microstrip transmission lines. They derived an empirical relation to account for the variation of the phase velocity in a 50 ohm microstrip transmission line on .025 inch thick alumina substrates ($\varepsilon_r = 9.6$) over the frequency range of 1GHz to 18GHz. Their empirical relation can predict dispersion only in the above mentioned microstrip transmission line and so is of little practical use.

In December 1969, Arnold[6] reported dispersion measurement results for microstrip transmission lines at frequencies in the range

---

* In analytical and numerical solutions a large conducting box enclosing the microstrip transmission line is required in order to satisfy the boundary conditions.

of 1GHz to 15GHz. He derived an empirical relation which may be used to calculate the variation of the effective dielectric constant of microstrip transmission lines with frequency. This equation is valid for lines on .025 inch thick alumina substrates with $\frac{w}{h}$ ratios of less than or equal to two. However, it does not predict dispersion for any other substrate and/or any other thickness or for $\frac{w}{h}$ ratios greater than two.

In October 1970, Grunberger et al[7] reported a numerical analysis of dispersion, in which all the components of the electric and magnetic fields and the propagation coefficient β were described in terms of power series of frequency ω. The higher order terms represent the correction to be added to the low frequency solutions in order to obtain the field patterns of microstrip transmission lines at high frequencies. Electric and magnetic field strengths were measured with a probe on the surface of the outer conductor of a microstrip transmission line enclosed in a box. The computed results show good agreement with experimental results on a microstrip transmission line with $\varepsilon_r = 2.89$, h = 4.5 cms, $\frac{w}{h} = 2.2$ and box dimensions as 21 cms x 30 cms. However, this approach requires a measurement of the electric and magnetic fields and the application of computer based curve fitting techniques and so is of little practical use.

Recently, in December 1970, Davis et al[8] reported a computer analysis (based on finite difference methods) of dispersion in microstrip transmission lines enclosed in a large conducting box. The computed results are in good agreement with the measured dispersion data on a microstrip transmission line with $\varepsilon_r = 9.7$, $\frac{w}{h} = 1$ and h = 50 mils.

The analysis confirmed the existance of higher order modes. These higher modes were found to be very similar to surface wave modes. However, the analysis requires extensive computation and a large computer memory and as such is not convenient to calculate dispersion in microstrip transmission lines.

1.4 Thesis Objectives and Approach

As was shown in the previous section, dispersion in microstrip transmission lines has been studied using the following approaches:

i) Numerical[4,7, 8]

ii) Empirical[5,6]

iii) Analytical[1]

The numerical analysis described by various authors[4,7, 8] require difficult and lengthy computer calculations and moreover, fail to provide insight into the dominant physical phenomenon. For these reasons, this approach is not convenient for the purpose of microstrip component design and is not considered in this thesis. The empirical and analytical results reported to date describe dispersion only for specific cases of microstrip transmission lines[1,5,6] (i.e. specific ε_r, h and $\frac{w}{h}$ ratios) and therefore, are not useful for design purpose.

The objective of this thesis is to find empirical and analytical relations which describe dispersive properties of microstrip transmission

lines for a wide range of microstrip transmission line parameters of interest. These relations are required in a form convenient for the purpose of microstrip component design.

Empirical relations which are described in Chapter 2 of this thesis were developed from experimental results on dispersion by noting the trend of the variation of the effective dielectric constant with frequency as the parameters ε_r, h and $\frac{w}{h}$ are varied independently. The derived relations describe the variation of the effective dielectric constant with frequency (within $\pm$ 5%) for a wide range of microstrip transmission lines ($2 \leq \varepsilon_r \leq 10$, $0.9 \leq \frac{w}{h} \leq 13$, .02 inch $\leq h \leq$ .125 inch) and can be used to predict the frequency above which dispersion effects are significant. A description of the dispersion measurement techniques are given in the same chapter.

A coupled mode analysis considering the coupling of the TEM mode and the dominant surface wave mode (TM_o) is developed in Chapter 3 of this thesis. An expression for the coupling coefficient has been derived using a series of qualitative arguments and the experimental data from Chapter 2. It is shown that analytical and experimental results are in close agreement ($\pm$ 2%) for a wide range of microstrip transmission lines ($2 \leq \varepsilon_r \leq 104$, .020 inch $\leq h \leq$ 0.125 inch and $0.9 \leq \frac{w}{h} \leq 6$). A design example which demonstrates the application of the dispersion analysis developed in this thesis is also given in Chapter 3.

CHAPTER 2

QUANTITATIVE STUDY OF DISPERSION IN MICROSTRIP TRANSMISSION LINES

2.1 Introduction

The experimental technique used to measure dispersive effects in microstrip transmission lines is described in this chapter. Also, empirical relations which describe the dependence of ε_{eff} on frequency, ε_r, h and $\frac{w}{h}$ are developed using the author's own experimental results as well as those reported by Troughton[3]. The results given by the empirical relations are compared with experimental data and with the results predicted by Arnold's[6] empirically derived formula.

2.2 Dispersion Measurements in Microstrip Transmission Lines

The apparent variation of ε_{eff} with frequency (i.e. dispersion) can be determined experimentally be measuring the microstrip transmission line wavelength λ_m and applying the following relations:

$$\lambda_m = \frac{\lambda_a}{(\varepsilon_{eff})^{\frac{1}{2}}}$$

$$\varepsilon_{eff} = \left(\frac{\lambda_a}{\lambda_m}\right)^2 \quad \ldots\ldots \qquad 2.1$$

The wavelength λ_m may be determined using one of the two following methods:

2.2.1 Standing Wave Detection Method

The standing wave detection method consists of using a slotted line to determine the distance between two consecutive minima of the standing wave pattern in a transmission line.[21,22] The distance between two consecutive minima is equal to half a wavelength. The measurement may be made on a microstrip transmission line by connecting a short circuited microstrip transmission line as a load to a coaxial slotted line. In such an arrangement, Figure 9, a movement of the short circuit on the microstrip transmission line will cause an equivalent (electrical length) movement or shift of minimas in the coaxial slotted line. Thus by measuring the movement of the short on the microstrip transmission line and the corresponding shift in minima on the slotted line, one can determine the wavelength on the microstrip transmission line as shown below:

With ℓ_m, ℓ'_m, ℓ_c and ℓ'_c defined as in Figure 9:

$$\frac{\ell_c}{\lambda_c} + \frac{\ell_m}{\lambda_m} = \frac{\ell'_c}{\lambda_c} + \frac{\ell'_m}{\lambda_m}$$

or

$$\frac{\ell'_c - \ell_c}{\lambda_c} = \frac{\ell_m - \ell'_m}{\lambda_m}$$

i.e.

$$\lambda_m = \frac{\ell_m - \ell'_m}{\ell'_c - \ell_c}\,\lambda_c \quad \ldots\ldots \qquad 2.2$$

The above procedure, however, suffers from the following disadvantages:

(a) It is difficult to establish a movable short circuit.

(b) The connectors available for transition of a microstrip transmission line to a coaxial line are mismatched and the reflection coefficient varies with frequency[5]. This mismatch results in a shift of minimas of the standing wave patterns on the slotted line in addition to the shift caused by the movement of the short on the microstrip transmission line and hence introduces a measurement error.

2.2.2 Resonance Method

The resonance method, first suggested by Troughton[3] and recently used by various other authors[6,23], consists of measuring the resonant frequency of a transmission line resonator of the type shown in Figure 7. This ring structure gives maximum power transmission at a frequency (defined as the resonant frequency) at which the mean circumference of the ring equals an integral multiple of the wavelength of the propagating microstrip transmission line mode. Thus at resonance,

$$\pi D_{mean} = n\lambda_{mr}$$

or

$$\lambda_{mr} = \frac{\pi D_{mean}}{n}$$

$$= \frac{\pi(2R + w)}{n} \quad \ldots\ldots \qquad 2.3$$

where n is an integer and λ_{mr} is the wavelength of the propagating microstrip transmission line mode at the nth resonant frequency.

Combining equations 2.1 and 2.3

$$\varepsilon_{eff} = \left[\frac{n}{\pi(2R+w)} \frac{c}{f_{mr}} \right]^2 \quad \ldots\ldots \qquad 2.4$$

This method offers the following advantages over the standing wave detection method:

(i) No short circuit is required.

(ii) By using a suitable ring resonator (as discussed in the next section), the effect of the coaxial-microstrip adaptors is minimized.

This method has been used in this thesis for the measurement of the effective dielectric constant of microstrip transmission lines. The measurement technique, results and experimental errors are discussed in the following section.

2.2.2.a Measurement Technique and Results

A microwave bridge of the form shown in Figure 10 (HP Network Analyser, Model 8410A) was used to conduct the transmission measurements. The input microwave signal is swept over a range of frequencies and the resulting output resonance curve observed on the C.R.O screen. The effective dielectric constant of the microstrip transmission line is calculated by substituting the value of the resonant frequency in

Equation 2.4, the other quantities in Equation 2.4 being known from the dimensions of the ring structure.

The resonant frequency of the ring cavity is dependent on the degree of coupling between the ring and the coupling probes[24]. The effect of the coupling probes is minimized by taking a large ring resonator (about five wavelengths long at the frequency of interest) and a coupling gap width which gives maximum Q of the cavity coupling structure[3]. The loaded quality factor of the coupled transmission line resonator is determined by measuring the half power band width (Δf_{mr}) and the resonant frequency (f_{mr})[24]:

$$Q_L = \frac{f_{mr}}{\Delta f_{mr}} \quad \ldots \qquad 2.5$$

The variation of Q_L versus coupling gap widths is plotted in Figure 11. The decrease in Q_L for larger gaps (more than 10 mils) is due to the power lost by radiation from the cavity (see Appendix A).

Using microstrip transmission line ring resonators with optimum coupling gap widths, the effective dielectric constants for various microstrip transmission lines with difference $\frac{w}{h}$ ratios on three different substrates (ε_r = 2.32, h = 30 mils; ε_r = 7.0, h = 20 mils; ε_r = 9.25, h = 125 mils) were measured and the results are plotted in Figures 12 to 15. These results indicate that dispersion is particularly significant for thick substrates with high relative dielectric constants and is more pronounced for wider lines.

2.2.2.b Measurement Error

The errors in the measurement of the effective dielectric constant and the quality factor of the transmission microstrip cavity are due to errors in the measurement of resonant frequency, f_{mr}, and the half power bandwidth. The error in f_{mr} is estimated to be of the order of $\pm$ 20 MHz while the bandwidth error is estimated to be of the order of $\pm$ 1 MHz for small gaps (less than 10 mils). For larger gaps the error is more since the transmitted signal is weak and may be below the dynamic range of the detecting instruments. These factors may introduce an error of $\pm$ 0.4% in the calculated value of the effective dielectric constant and an error of $\pm$ 5% (for small gaps) to $\pm$ 10% (for large gaps) in the value of Q_L as shown in Figure 11.

2.3 Empirical Relations for Dispersion in Microstrip Transmission Lines

The experimental results presented in the previous section (and by other authors[1-6]) indicate that the effective dielectric constant is frequency dependent above S band (2-4 GHz) frequencies. Empirical relations are developed in this section following a brief description of the empirical equations derived by other authors[5,6]. A coupled mode analysis of dispersion is developed in the subsequent chapter.

Napoli and Hughes[5] derived the following empirical equation from their experimental observations:

$$\varepsilon_{eff} = \varepsilon_{eff_o}\left[1 + \left(\frac{f}{f_\beta}\right)^2\right]^2 \qquad 2.6$$

where f_β = 59 GHz.

This relation was derived from the dispersion measurements on a 50 ohm microstrip transmission line with a .025 inch thick alumina (ε_r = 9.6) substrate and is not valid for any other substrate material, substrate thickness or $\frac{w}{h}$ ratio.

Arnold[6] derived the following empirical relation:

$$\frac{v}{c} = A\left[1.15\left(\frac{w}{h}\right)^{0.211}\varepsilon_{dc}^{2.04} f \times 10^{-5}\right] \qquad 2.7$$

where

v = phase velocity of the wave on the microstrip transmission line

c = velocity of light in free space

$\frac{v}{c} = \left(\varepsilon_{eff}\right)^{\frac{1}{2}}$

ε_{dc} = relative permitivity of the substrate material at zero frequency

f = frequency in GHz

and

A = value of $\frac{v}{c}$ computed from $0.986\ \varepsilon_{dc}$.

This relation may be used to calculate $\varepsilon_{eff} = \varepsilon_{eff}(f)$ for microstrip transmission lines having $\frac{w}{h}$ ratios up to two on an alumina substrate of thickness .025 inch and dielectric constant of the order of 9.9 (see Figures 12 to 15).

These empirical relations (2.6 and 2.7) are of limited practical use since they fail to predict the dispersive behaviour in microstrip transmission lines for a wide variety of ε_r, h and $\frac{w}{h}$ ratios. In the remainder of this section, empirical relations are developed which describe the dispersive properties of microstrip transmission lines for a wide range of parameters ($2 \leq \varepsilon_r \leq 10$, 20 mils $\leq h \leq$ 50 mils, $0.9 \leq \frac{w}{h} \leq 13$). The relations were developed by noting the trends of the variation of the effective dielectric constant with frequency as the parameters ε_r, h and $\frac{w}{h}$ ratio are varied independently:

(i) $\frac{\partial \varepsilon_{eff}}{\partial f}$ is strongly dependent on the dielectric constant of the substrate material and increase approximately as the square of the relative dielectric constant and is zero for an air dielectric. This gives

$$\frac{\partial \varepsilon_{eff}}{\partial f} \quad \alpha \quad (\varepsilon_r^2 - 1)$$

(ii) $\frac{\partial \varepsilon_{eff}}{\partial f}$ is dependent on the characteristic impedance of the microstrip transmission line and $\frac{w'}{h}$* ratio. For various combinations of Z_o and $\frac{w'}{h}$, it was observed that

$$\frac{\partial \varepsilon_{eff}}{\partial f} \quad \alpha \quad \left(Z_o \quad \frac{w'}{h}\right)^{\frac{1}{2}} \quad \text{for } \frac{w'}{h} \leq 4$$

and

$$\frac{\partial \varepsilon_{eff}}{\partial f} \quad \alpha \left\{ \frac{Z_o}{3} \quad \left(\frac{w'}{h}\right)^2 \right\}^{\frac{1}{2}} \quad \text{for } \frac{w'}{h} > 4$$

* The finite thickness of the metallization of the strip conductor serves to increase the effective width of the line to a value slightly greater than the actual physical width[14].

(iii) $\frac{\partial \varepsilon_{eff}}{\partial f}$ is linearly dependent on the substrate thickness:

$$\frac{\partial \varepsilon_{eff}}{\partial f} \alpha h \quad .$$

(iv) $\frac{\partial \varepsilon_{eff}}{\partial f}$ is significant only above a certain frequency, f_o. Above this frequency the variation of ε_{eff} with frequency is approximately linear. The frequency f_o is found from experimental results to be dependent on ε_r, Z_o and h in the following manner:

a) $f_o \alpha (Z_o)^{\frac{1}{2}}$

b) $f_o \alpha (\varepsilon_r - 1)^{-\frac{1}{4}}$

c) $f_o \alpha (h)^{-\frac{1}{2}}$ 2.8

Therefore $f_o = \frac{K_1}{(\varepsilon_r - 1)^{\frac{1}{4}}} \left(\frac{Z_o}{h}\right)^{\frac{1}{2}}$ 2.9

where f_o is in GHz and K_1 is a constant to be determined experimentally.

From the above observations, for $f \geq f_o$:

$$\varepsilon_{eff} = K_2 (\varepsilon_r^2 - 1) h (Z_o \frac{w'}{h})^{\frac{1}{2}} (f-f_o) + \varepsilon_{eff_o} \text{ for } \frac{w'}{h} \leq 4 \qquad 2.10$$

and

$$\varepsilon_{eff} = K_2 (\varepsilon_r^2 - 1) h \left\{ \frac{Z_o}{3} \left(\frac{w'}{h}\right)^2 \right\}^{\frac{1}{2}} (f-f_o) + \varepsilon_{eff_o} \text{ for } \frac{w'}{h} > 4 \qquad 2.11$$

where f is the frequency in GHz and h is mils. The constants K_1 and K_2 were determined experimentally to be 6.0 and 3×10^{-6} respectively. Therefore we have

$$f_o = \frac{6.0}{(\varepsilon_r - 1)^{\frac{1}{4}}} \left(\frac{Z_o}{h}\right)^{\frac{1}{2}} \qquad 2.12$$

$$\varepsilon_{eff} = 3 \times 10^{-6} (\varepsilon_r^2 - 1)\, h\, (Z_o \frac{w'}{h})^{\frac{1}{2}} (f-f_o) + \varepsilon_{eff_o} \text{ for } \frac{w'}{h} \leq 4,\ f \geq f_o \qquad 2.13$$

and

$$\varepsilon_{eff} = 3 \times 10^{-6} (\varepsilon_r^2 - 1)\, h \left\{\frac{Z_o}{3} \left(\frac{w'}{h}\right)^2\right\}^{\frac{1}{2}} (f-f_o) + \varepsilon_{eff_o} \text{ for } \frac{w'}{h} > 4,\ f \geq f_o \qquad 2.14$$

where f and f_o are in GHz and h is in mils. ε_{eff_o} = static effective dielectric constant (determined from Wheeler's curve 16a and 16b).

The results calculated from these empirical relations are superimposed on Figures 12 to 15 along with the results from Arnold's empirical equation. It is observed that the empirical relations derived in this thesis describe accurately (within $\pm$ 5%) the apparent variation of the effective dielectric constant with frequency for a wide range of dielectric constants ($2 \leq \varepsilon_r \leq 10$), $\frac{w}{h}$ ratios ($0.9 \leq \frac{w}{h} \leq 13$) and substrate thicknesses (.020 inch $\leq h \leq$ .125 inch).

The f_o term in equations 2.13 and 2.14 is particularly useful in practice since it enables one to predict the frequency at which dispersion becomes significant as the microstrip transmission line parameters h, $\frac{w}{h}$ and ε_r are varied independently.

CHAPTER 3

A COUPLED MODE ANALYSIS OF DISPERSION IN MICROSTRIP TRANSMISSION LINES

3.1 Introduction

In the previous chapter, empirical relations were developed which describe the variation of effective dielectric constant for microstrip transmission lines with frequency. The results predicted by these relations are in close agreement with the experimental values. However, to acquire an understanding of the physics of the dispersion phenomenon, an analytical approach is required. In this chapter an approach is developed which combines an approximate closed form solution with a series of qualitative arguments (all of which provide physical insight to the problem). The approach is based on an analysis of the coupling between the TEM mode and the transverse surface wave modes due to the air dielectric interface[1,10,20,27]. Hartwig et al[1] and Vendelin[20] reported that the field components for a TM surface wave mode coincide with the TEM mode and may be easily excited, as opposed to a TE surface wave mode whose field components are in quadrature with the TEM mode. For a microstrip geometry only even TM and odd TE surface wave modes are possible, since for even TE and odd TM surface wave modes the electric field does not vanish along the ground plane[28] (see Appendix B). It is easily seen (Appendix B)

that the TM_o mode is dominant since it has a zero cut off frequency while higher order modes have cut off frequencies beyond the range of interest and therefore have negligible effects. This reasoning is employed in this chapter in the development of expressions for the upper frequency limit of microstrip transmission lines and expressions which describe the apparent variation of the effective dielectric constant with frequency and microstrip geometry at frequencies below the upper frequency limit.

3.2 Upper Frequency Limit on the Operation of Microstrip Transmission Lines

The TM_o mode may couple with the TEM mode and hence change the transmission behaviour[29] (i.e. the propagation constant) of the microstrip transmission line. As the frequency increases, the phase velocity of the TM_o mode decreases (see Figure B.1). Thus the effect of coupling of the TM_o mode with the TEM mode is more pronounced at higher frequencies, since the coupling is inversely dependent on the phase velocity[20]. The frequency at which the phase velocity of the TM_o mode is equal to the phase velocity of the TEM mode has been defined[1] as the upper frequency limit. Vendelin derived the following expression for the upper frequency limit for very narrow lines:

$$f_{\ell n} = \frac{c}{2\pi h} \sqrt{\frac{2}{\varepsilon_r - 1}} \arctan \varepsilon_r \qquad 3.1$$

Based on a similar approach, the following general expression is developed in this thesis (see Appendix B - D) which may be used to calculate the upper frequency limit for any $\frac{w}{h}$ ratio[32]:

$$f_\ell = \frac{c}{2\pi h}\,\frac{2}{\sqrt{\varepsilon_r - 1}}\left[1 - \left(1 + 10\,\frac{h}{w}\right)^{-\frac{1}{2}}\right]^{-\frac{1}{2}} \arctan\,\varepsilon_r \left[\frac{1 + \left(1 + 10\,\frac{h}{w}\right)^{-\frac{1}{2}}}{1 - \left(1 + 10\,\frac{h}{w}\right)^{-\frac{1}{2}}}\right]^{\frac{1}{2}} . \qquad 3.2$$

This expression reduces to 3.1 for $\frac{w}{h} = 0$.

Values of f_ℓ given by equation 3.2 are plotted in Figure 18. For $\frac{w}{h} << 1$ and $\varepsilon_r > 10$, equation 3.1 and 3.2 reduces to[8]

$$f_{\ell_n} \simeq \frac{10.6}{h\sqrt{\varepsilon_r}} \quad \text{GHz} \qquad 3.3$$

and is convenient for preliminary calculations.

3.3 Coupled Mode Analysis of Dispersion

Hartwig et al[1] developed an analysis of the dispersive behaviour of microstrip transmission lines below the upper frequency limit, f_ℓ, by considering the coupling of the TEM and TM_o modes. Coupled mode theory[1,29] gives (see appendix B and C):

$$\varepsilon_{\text{eff}_{1,2}} = \left[\frac{\sqrt{\varepsilon_{\text{eff}_o}} + \sqrt{\varepsilon_{\text{eff}_{TM_o}}}}{2} \pm \sqrt{\frac{\varepsilon_{12}}{\xi}\cdot\frac{\varepsilon_{21}}{\xi}\cdot\xi^2 + \left\{\frac{\sqrt{\varepsilon_{\text{eff}_o}} - \sqrt{\varepsilon_{\text{eff}_{TM_o}}}}{2}\right\}^2}\right]^2 \qquad 3.4$$

where

$\varepsilon_{\text{eff}_1}$ = effective dielectric constant of the dispersive microstrip (Mode 1, + sign)

$\varepsilon_{\text{eff}_2}$ = effective dielectric constant of the dispersive microstrip (Mode 2, - sign)

$\varepsilon_{\text{eff}_o}$ = static effective dielectric constant of the microstrip line (determined from Wheeler's curve, Figs. 16a and 16b)

$\varepsilon_{eff_{TM_o}}$ = effective dielectric constant of the TM_o mode (determined graphically, Figures 19-23)

For passive coupling, reciprocity holds and the coupling coefficients $\frac{\varepsilon_{12}}{\xi}$ and $\frac{\varepsilon_{21}}{\xi}$ are equal, i.e.

$\frac{\varepsilon_{12}}{\xi} = \frac{\varepsilon_{21}}{\xi}$ = coupling coefficient between assumed TEM mode and TM_o mode

$\xi^2 = \left(\varepsilon_{eff_o} \cdot \varepsilon_{eff_{TM_o}}\right)^{\frac{1}{2}}$ is the normalizing factor.

$\varepsilon_{12} \cdot \varepsilon_{21} = \varepsilon_{12}^2$ is the only unknown quantity on the right hand side of equation 3.4. A theoretical derivation of ε_{12}^2 is not possible without an explicit description of the electric and magnetic fields of the TEM mode. Hartwig et al[1] derived two different empirical equations for ε_{12}^2 to fit experimentally determined dispersion data for an alumina substrate (ε_r = 9.7, h = 50 mils, $\frac{w}{h}$ = 0.96) and for a rutile substrate (ε_r = 104, h = 50 mils, $\frac{w}{h}$ = 0.6) respectively. The expressions derived by Hartwig et al[1] are of limited practical interest since they can not be used to predict the dispersion properties of microstrip transmission lines having different $\frac{w}{h}$ ratios, substrate thickness, or dielectric constant.

An expression for ε_{12}^2 is developed in this thesis from the following series of arguments[32]:

1) Coupling may be assumed to be inversely dependent on the phase velocities of the TEM and TM_o modes, the phase velocities for both these modes being inversely dependent on the substrate

dielectric constant. Thus we may initially assume

$$\varepsilon_{12}^2 \alpha \frac{1}{(V_{ph})^{n_1}} \alpha (\eta)^{n_1} \qquad 3.5$$

where $\eta = \sqrt{\varepsilon_r}$ is the refractive index of the substrate material and n_1 is a constant. Since the phase velocities of both the TM_o and TEM modes depend on η, we assume that $n_1 = 2$. In practice one observes that dispersion decreases rapidly as the dielectric constant of the substrate decreases and is in fact zero for $\eta = 1$. To take this into account we finally assume that

ε_{12}^2 varies as $(\eta - 1)^2$ instead of η^2, i.e.

$$\varepsilon_{12}^2 \alpha (\eta - 1)^2 \qquad 3.6$$

2) Coupling between TM_o and TEM modes above the upper frequency limit f_ℓ is large and increases rapidly with frequency, so we may assume

$$\varepsilon_{12}^2 \alpha \left(\frac{f}{f_\ell}\right)^{n_2} \qquad 3.7$$

where $n_2 > 1$ and is determined from experimental results on dispersion.

3) The phase velocity of the TEM microstrip line mode is inversely dependent on $\frac{w'}{h}$ ratio[14], so we may assume

$$\varepsilon_{12}^2 \alpha \left(\frac{w'}{h}\right)^{n_3} \qquad 3.8$$

where n_3 is to be determined from experimental results.

Combining 3.6, 3.7 and 3.8 we have

$$\varepsilon_{12}^2(f) = k(\eta - 1)^2 \left[\frac{w'}{h}\right]^{n_3} \left[\frac{f}{f_\ell}\right]^{n_2} \qquad 3.9$$

where k is a constant to be determined.

Combining equations 3.4 and 3.9 we have (Appendix C):

$$\left[\sqrt{\varepsilon_{eff_1}} - \frac{\sqrt{\varepsilon_{eff_o}} + \sqrt{\varepsilon_{eff_{TM_o}}}}{2}\right]^2 - \left[\frac{\sqrt{\varepsilon_{eff_o}} - \sqrt{\varepsilon_{eff_{TM_o}}}}{2}\right]^2 = \varepsilon_{12}^2 \qquad 3.10$$

(In this equation only ε_{eff_1} (mode 1) has been considered, the reason for this will become evident from the discussion given later.)

or

$$\text{L.H.S.} = X(f_m) = k(\eta - 1)^2 \left[\frac{w'}{h}\right]^{n_3} \left[\frac{f_m}{f_\ell}\right]^{n_2} \qquad 3.11$$

where for a given microstrip, $X(f_m)$ can be calculated from experimental results on dispersion. Since n_2, n_3 and k are independent of frequency, the average value of n_2, n_3 and k, for a range of frequencies of interest, can be found respectively from the following expressions (See Appendix E):

$$n_2 = \frac{1}{N-1} \sum_{m=2}^{m=N} \frac{\log\{X(f_m)/X(f_{m-1})\}}{\log(f_m/f_{m-1})} \qquad 3.12$$

$$n_3 = \frac{1}{N} \sum_{m=1}^{m=N} \frac{\log \left\{ X(f_m) \cdot (f_\ell)^{n_2} \right\}_{\frac{w'}{h} = x} - \log \left\{ X(f_m) \cdot (f_\ell)^{n_2} \right\}_{\frac{w'}{h} = y}}{\log \left\{ \frac{x}{y} \right\}} \qquad 3.13$$

and

$$k = \frac{1}{N} \sum_{m=1}^{m=N} \frac{X(f_m)}{(\eta - 1)^2 \left[\frac{w'}{h} \right]^{n_3} \left[\frac{f_m}{f_\ell} \right]^{n_2}} \qquad 3.14$$

where N is any integer > 1.

The calculated values of n_2, n_3 and k were found to be $\frac{4}{3}$, $\frac{3}{4}$ and 0.22 respectively, subsequently

$$\varepsilon_{12}^2 = 0.22 \, (\eta - 1)^2 \left[\frac{w'}{h} \right]^{\frac{3}{4}} \left[\frac{f}{f_\ell} \right]^{\frac{4}{3}} \qquad 3.15$$

The values of ε_{eff_1}, which have been calculated substituting equation (3.15) into equation (3.4) for various microstrip lines with different ε_r, h and $\frac{w}{h}$ are plotted in Figures 24 to 28 along with the experimental results. The theoretical and experimental results agree within $\pm$ 2.0%.

Equation (3.4) gives two roots (or modes) for ε_{eff}. However, for frequencies $f \lesssim 0.5f_\ell$ the value of ε_{eff_2} computed from equation (3.4) is less than unity, and as such, may be disregarded. At frequencies $f \gtrsim 0.5f_\ell$ both modes ε_{eff_1} and ε_{eff_2} exist and have different phase velocities. It is believed that this phenomena has been observed while conducting measurements with a resonant ring[3] on a thick (h = 125 mils)

substrate (ε_r = 9.25, f_ℓ = 13.05 GHz). It was observed that above 7 GHz, more than twice the expected number of resonance peaks appeared in the resonance response of the ring resonator. These extra peaks in the resonance response may be due to the existence of the ε_{eff_2} mode and other modes (TE_1 surface wave modes and transverse resonance modes[20]) which may also appear at such high frequencies.

In summary, a coupled mode analysis of dispersion in microstrip transmission lines has been reported in this Chapter. The analysis describes the coupling of the TEM mode and the TM_o mode and may be used to describe the dispersive properties of a wide range of microstrip configurations ($2 \leq \varepsilon_r \leq 104$, .025 inch $\leq h \leq$ .125 inch; and $0.9 \leq \frac{w}{h} \leq 6$) up to frequencies as high as $0.5f_\ell$. The analysis and experimental results both indicate that additional coupled modes may exist at frequencies above $0.5f_\ell$. In the following section a design example is given which demonstrates the application of the coupled mode analysis as well as the empirical model developed in Chapter 2 of this thesis.

3.4 A Design Example

The problem chosen consists of the design of a quarter wave transformer to match a 50 ohm load (Z_L) to a 8 ohm load (Z_{in}) at 10GHz using a ceramic powder-filled polstyrene material (ε_r = 7.0) of thickness h = 20 mils (see Figure 29).

The characteristic impedance of a quarter wave transformer is given by[22]

$$Z_{02} = \left(Z_L \, Z_{in}\right)^{\frac{1}{2}}$$

For Z_L = 50 ohms and Z_{in} = 8 ohms

$$Z_{02} = 20 \text{ ohms}$$

For a given ε_r and h, the characteristic impedance of a microstrip transmission line is determined by the width of the strip conductor. Thus, for the design of a transformer, the quantities to be determined are the width and the length of the strip conductor. These quantities are determined from various approaches as described below:

A. Wheeler's Solutions (i.e. Low Frequency Approximation)[14]

From Wheeler's curve (Figures 16a and 16b) for the given ε_r = 7 and Z_{002} = 20 ohms, one finds $\frac{w}{h}$ and $\frac{\lambda_a}{\lambda_{mo}}$ to be 5.6 and 2.30 respectively.

Therefore

$$\lambda_{mo} = \frac{\lambda_a}{2.39}$$

$$= \frac{3}{2.39} = 1.2552 \text{ cms at 10GHz}$$

Hence

length of the transformer = $\frac{\lambda_{mo}}{4}$ = 0.3138 cm

width of the transformer = 5.6h = 0.284 cm

B. Empirical Model (Chapter 2)

From equation 2.1

$$\lambda_m = \frac{\lambda_a}{(\varepsilon_{eff})^{\frac{1}{2}}}$$

For $\frac{w}{h} = 5.6$, $\varepsilon_r = 7.0$, h = 20 mils and t = 1.3 mils, ε_{eff} is found to be 5.9748 from equations 2.12 and 2.14.

Therefore

$$\lambda_m = \frac{3}{(5.9748)^{\frac{1}{2}}} = 1.2273 \text{ cms. at 10GHz}$$

Hence

length of the transformer = $\frac{\lambda_m}{4}$ = 0.3068 cm.

width of the transformer = 5.6 h = 0.284 cm.

C. Coupled Mode Model (Chapter 3)

The effective dielectric constant of a microstrip transmission line is found by substituting f_ℓ, ε_{12}^2 and $\varepsilon_{eff_{TM_o}}$ in equation 3.4 for $\frac{w}{h} = 5.6$, $\varepsilon_r = 7.0$, h = 20 mils and t = 1.3 mils, f_ℓ and ε_{12}^2 are found to be 129GHz and .07265 respectively using equations 3.2 and 3.15.

β_{TM_o} is found by substituting the value of p_d in equation B.7, where p_d is determined graphically by plotting equations B.13 and B.14 in a $p_d h$, $p_a h$ plane as shown in Figure 20 and noting the point of intersection of the two curves at the given frequency. For this example,

f = 10GHz, the point of intersection of the two curves in Figure 20 gives:

$$p_d h = .26 \text{ radians}$$

Therefore

$$p_d = \frac{.26}{h} = 5.1181 \text{ radians/cm}$$

From equations B.7 and B.20,

$$\varepsilon_{eff_{TM_o}} = \left(\frac{\beta_{TM_o}}{\beta_a}\right)^2 = \varepsilon_r - \frac{p_d^2}{\beta_a^2} = 1.03619 \text{ at 10GHz}$$

where

$$\beta_a^2 = \frac{4\pi^2}{\lambda_a^2} = 4.39234 \text{ at 10GHz}$$

Substituting f_ℓ, ε_{12}^2 and $\varepsilon_{eff_{TM_o}}$ in equation 3.4,

$$\varepsilon_{eff} = 5.9587$$

Therefore $$\lambda_m = \frac{\lambda_a}{(\varepsilon_{eff})^{\frac{1}{2}}}$$

$$= \frac{3}{(5.9587)^{\frac{1}{2}}} = 1.229 \text{ cms. at 10GHz}$$

Hence

$$\text{length of the transformer} = \frac{\lambda_m}{4} = .3072 \text{ cm}$$

$$\text{width of the tranformer} = 5.6h = 0.284 \text{ cm}$$

D. Empirical Model with Dispersion of Z_o Included

The calculations performed in B and C take into account the variation of the effective dielectric constant with frequency, but neglect the variation of the characteristic impedance with frequency. Napoli et al[5] reported experimentally derived curves for the variation of $\frac{\beta - \beta_o}{\beta_o}$ and $\frac{Y_o - Y_{oo}}{Y_{oo}}$ with frequency for $\varepsilon_r = 9.6$. It is observed that the slope of the $\frac{Y_o - Y_{oo}}{Y_{oo}}$ curve is approximately three times the slope of the $\frac{\beta - \beta_o}{\beta_o}$ curve. Thus we may write

$$\frac{\beta - \beta_o}{\beta_o} = m_1(f - f_o) \qquad 3.16$$

and

$$\frac{Y_o - Y_{oo}}{Y_{oo}} = 3m_1(f - f_o) \qquad 3.17$$

where m_1 is a constant depending on ε_r, h and $\frac{w'}{h}$.

In order to find an expression of m_1, we rewrite equation 3.16 in the form of equation 2.13 or 2.14:

$$\beta = \beta_o (1 + m_1 f')$$

where

$$f' = (f - f_o) \text{ GHz}$$

therefore

$$\left(\frac{\beta}{\beta_a}\right)^2 = \left(\frac{\beta_o}{\beta_a}\right)^2 \quad (1 + m_1 f')^2$$

or

$$\varepsilon_{eff} = \varepsilon_{eff_o} \left\{ 1 + 2m_1 f' + (m_1 f')^2 \right\}$$

$$\simeq \varepsilon_{eff_o} (1 + 2m_1 f')$$

where it is assumed that $m_1 f' << 1$ (it is shown later that $m_1 f$ is of the order of .01).

Comparing the above equation with 2.13 and 2.14 and solving for m_1, we have

$$m_1 = \frac{3 \times 10^{-6} \ (\varepsilon_r^2 - 1) \ h \ (Z_o \frac{w'}{h})^{\frac{1}{2}}}{2 \ \varepsilon_{eff_o}} \quad \text{for } \frac{w'}{h} \leq 4 \qquad 3.18$$

and

$$m_1 = \frac{3 \times 10^{-6} \ (\varepsilon_r^2 - 1) \ h \left\{ \frac{Z_o}{3} \left(\frac{w'}{h} \right)^2 \right\}^{\frac{1}{2}}}{2 \ \varepsilon_{eff_o}} \quad \text{for } \frac{w'}{h} > 4 \qquad 3.19$$

For $\varepsilon_r = 7$, $h = 20$ mils, $Z_{oo} = 50$ ohms, $\frac{w}{h} = 1.3$, $t = 1.3$ mils and $\varepsilon_{eff_o} = 5.0176$,

$$m_1 = .00218 \text{ (equation 3.18)}$$

and

for the same substrate material with $Z_{oo2} = 20$ ohms and $\frac{w}{h} = 5.6$

$$m_1 = .003709 \text{ (equation 3.19)}$$

Equation 3.17 may be rewritten as

$$Y_o = Y_{oo} (1 + 3m_1 f') \qquad 3.20$$

or

$$Z_o = Z_{oo} (1 + 3m_1 f')^{-1} \qquad 3.21$$

or

$$Z_o = Z_{oo} (1 - 3m_1 f') \text{ for } m_1 f' << 1 \qquad 3.22$$

To obtain a first approximation of the width of the transformer, we assume that $Z_{oo2} = Z_{o2} = 20$ ohms. The corresponding value of $\frac{w}{h}$ from Wheeler[14] is 5.6.

Applying this value of $\frac{w}{h}$ in equations 3.19 and 3.21

$$Z_{oo2} = 20 [1 + 3(.003709)(6.2)] = 21.37 \text{ ohms.}$$

From Wheeler's curve for $Z_{oo2} = 21.37$ ohms, $\frac{w}{h} = 5.4$.

Using this value of $\frac{w}{h}$ in equations 3.19 and 3.21

$$Z_{oo2} = 20[1 + 3(.003634)(6.2)] = 21.35 \text{ ohms}$$

which agrees closely with the previous value and therefore we conclude that one iteration is sufficient.

Therefore

width of the transformer = $5.4h$ = 0.2743 cm.

length of the transformer = $\frac{\lambda_m}{4}$ = 0.3068 cm.

The length of the transformer is the same as calculated in B.

It should be mentioned that the above analysis of the frequency dependence of the characteristic impedance is only approximate and as is shown in the subsequent section, there remains a definite requirement for an analysis of the frequency dependence of the characteristic impedance.

3.4.1 Experimental Verification

To compare the validity and accuracy of the various approaches outlined in the previous section and to obtain an indication of the frequency dependence of the characteristic impedance, the structure* shown in Figure 30 was fabricated and the input impedance, Z_{in1}, determined experimentally (Z_{in} = 7.0 - j 2.0 ohms). The line widths and lengths were measured and the input impedance Z_{in} calculated from the various approaches of the previous section as described below:

A. Wheeler's[14] Solution (i.e. Low Frequency Approximation)

λ_{m1} = 1.34 cms

Z_{o1} = 50 ohms

$\frac{\ell_1}{\lambda_{m1}}$ = .04965

$\frac{\ell_3}{\lambda_{m3}}$ = .7485

λ_{m2} = 1.2552 cms

Z_{o2} = 20 ohms

$\frac{\ell_2}{\lambda_{m2}}$ = .2247

Z_L = 50 ohms

*Note this structure was not designed using the computations of the previous section. Instead a structure of arbitrary dimensions (but resembling a quarter wave transformer) was fabricated and the measured line widths and lengths used to calculate the input impedance with the aid of the various models described in the previous section.

Therefore

$$Z_{in1} = 50(0.162 - j\ 0.072) \text{ ohms}$$

$$= 8.1 - j\ 3.6 \text{ ohms}$$

B. Empirical Model (Chapter 2)

$\lambda_{m1} = 1.321$ cms. $\qquad \lambda_{m2} = 1.2273$ cms.

$Z_{o1} = 50$ ohms $\qquad Z_{o2} = 20$ ohms

$\frac{\ell_1}{\lambda_{m1}} = 0.5035 \qquad \frac{\ell_2}{\lambda_{m2}} = 0.23$

$\frac{\ell_3}{\lambda_{m3}} = 0.759 \qquad Z_L = 50$ ohms

Therefore

$$Z_{in1} = 50(0.161 - j\ 0.022) \text{ ohms}$$

$$= 8.05 - j\ 1.1 \text{ ohms}$$

C. Coupled Mode Model (Chapter 3)

$\lambda_{m1} = 1.320$ cms. $\qquad \lambda_{m2} = 1.2290$ cms

$Z_{o1} = 50$ ohms $\qquad Z_{o2} = 20$ ohms

$\frac{\ell_1}{\lambda_{m1}} = 0.5038 \qquad \frac{\ell_2}{\lambda_{m2}} = 0.2294$

$\frac{\ell_3}{\lambda_{m3}} = 0.7591 \qquad Z_L = 50$ ohms

Therefore

$$Z_{in1} = 50(0.161 - j\ 0.02) \text{ ohms}$$

$$= 8.05 - j\ 1.0 \text{ ohms}$$

D. Empirical Model with Dispersion of Z_o Included

$\lambda_{m1} = 1.321$ cms

$\lambda_{m2} = 1.2273$ cms.

$Z_{o1} = 48.7$ ohms

$Z_{o2} = 18.6$ ohms

$\frac{\ell_1}{\lambda_{m1}} = 0.5035$

$\frac{\ell_2}{\lambda_{m2}} = 0.23$

$\frac{\ell_3}{\lambda_{m3}} = 0.759$

$Z_L = 50$ ohms (assumed constant)

Therefore

$$Z_{in1} = 48.7(0.151 - j\ 0.025) \text{ ohms}$$

$$= 7.35 - j\ 1.217 \text{ ohms}$$

In Summary:

$Z_{in1} = 7.0 - j\ 2.0$ ohms (Measured)

$Z_{in1} = 8.1 - j\ 3.6$ ohms (Approach A)

$Z_{in1} = 8.05 - j\ 1.1$ ohms (Approach B)

$Z_{in1} = 8.05 - j\ 1.0$ ohms (Approach C)

$Z_{in1} = 7.35 - j\ 1.2$ ohms (Approach D)

One observes that:

(i) The measured input impedance does not agree very well with the input impedances calculated from the various approaches.

(ii) The real part of the input impedance calculated using Approach D is closest to the measured result. This indicates that the characteristic impedances of the transmission lines of the structure shown in figure 30 are frequency dependent.

(iii) The imaginary portion of the input impedance is defined largely by ε_{eff}, therefore, these results demonstrate the frequency dependence of ε_{eff}. The imaginary portion of the input impedance given by approaches B, C and D are in close agreement with each other and differ by the measured value by an amount (1^{o} of arc on the Smith chart) which is of the order of the instrument errors*. It is seen that the value given by Wheeler's solutions[14] is approximately 2.6 ohms larger than that given by the dispersion models developed in this thesis. This is the expected behaviour since Wheeler's solutions give smaller value of ε_{eff} than the actual value at the measuring frequency.

---

*The quarter wave transformer was selected as the design example since it is a commonly used circuit element. The validity of the models developed in this thesis could have been more readily demonstrated using a $\frac{3\lambda_m}{8}$ transformer as this would have given Z_{in} values in a more expanded region of the Smith chart. However, further investigation of this matter was prevented by the time limitation.

The agreement between the measured and calculated characteristics of a transmission line depends on the accuracy with which the variation of Z_o and ε_{eff} with frequency is taken into account. It has been shown earlier that the variation of ε_{eff} with frequency is described adequately by the empirical and coupled mode models developed in this thesis and so the difference in the measured and the calculated characteristics is due to the variation of the characteristic impedance of the microstrip line with frequency. An accurate analysis of the variation of Z_o with frequency is currently not available in the literature and therefore, this should be the subject of further investigation.

CHAPTER 4

CONCLUSIONS AND RECOMMENDATIONS

4.1 Summation and Conclusions

The apparent variation of the effective dielectric constant of microstrip transmission lines with frequency (i.e. dispersion) has been considered in this thesis. Empirical and analytical models have been developed to study this variation:

(a) Empirical relations were developed from the experimental results on dispersion by studying the trend of the variation of the effective dielectric constant with frequency as the transmission line parameters ε_r (relative dielectric constant of the substrate), h (substrate thickness) and $\frac{w}{h}$ (width/thickness) ratio are varied independently. The derived relations account for the dispersion (within $\pm$ 5%) in microstrip transmission lines for a wide range of dielectric constants ($2 \leq \varepsilon_r \leq 10$), $\frac{w}{h}$ ratios ($0.9 \leq \frac{w}{h} \leq 13$) and substrate thickness (.020 inch $\leq h \leq$ .125 inch) and can be used to predict the frequency below which dispersion effects are negligible. Previously reported empirical relations[5,6] were valid only for specific cases of microstrip transmission lines (i.e. specific ε_r, h and $\frac{w}{h}$ ratio) while the empirical relations

derived in this thesis are of much more general nature. The relations are valid for frequencies at least as high as 13GHz.

(b) An analysis of the dispersive behaviour of microstrip transmission lines was developed by considering the coupling of the TEM and TM_o surface wave modes. Since a theoretical derivation of the coupling coefficient was not possible, due to the lack of an explicit description of electric and magnetic fields of the TEM mode, an expression for the coupling coefficient was derived from a series of qualitative arguments. The arguments were based on the assumption that coupling between TEM and TM_o modes is inversely dependent on the phase velocities of both the TEM and the TM_o modes. The phase velocities of these modes are a function of ε_r, h and $\frac{w}{h}$ and so the coupling of the modes can be related to the parameters ε_r, h and $\frac{w}{h}$ by analysing the experimentally determined dispersion data. The coupled mode analysis developed in this manner accurately describes (within $\pm$ 2%) the variation of effective dielectric constant of microstrip lines with frequency for a very wide range of microstrip configurations ($2 \leq \varepsilon_r \leq 104$; .02 inch $\leq$ h $\leq$ .125 inch; and $0.9 \leq \frac{w}{h} \leq 6$). The analysis and experimental results both indicate that additional coupled modes

may exist at frequencies above 0.5 f_ℓ, where f_ℓ is the frequency at which the phase velocities of both the TEM and TM_o surface wave modes are equal. This is considered to be the upper frequency limit for microstrip transmission lines. A general expression for f_ℓ, which is valid for microstrip transmission lines of any $\frac{w}{h}$ ratio is developed in this thesis.

The coupled mode model describe the dispersive behaviour in microstrip transmission lines over a wider range of dielectric constants and frequencies than the empirical model. However, for dielectric constants in the range, $2 \leq \varepsilon_r \leq 10$, and frequencies up to 13GHz, the empirical relations are more convenient for design purposes than are the coupled mode equations, as is evident from the design example in section 3.4.

The dispersion measurements were made using a resonant ring technique. Experimental, empirical and analytical results indicate that dispersion is more pronounced for higher dielectric constant substrates and/or thicker substrates and for wider lines. It is also shown that the characteristic impedance of microstrip transmission lines decreases with increasing frequency.

4.2 Recommendations for Future Work

The variation of the effective dielectric constant of microstrip transmission lines has been studied in this thesis while no detail attempt was made to thoroughly investigate the variation of the characteristic impedance and the attenuation constant of microstrip transmission lines with frequency. It is suggested that attention be given to these aspects of the high frequency characteristics of microstrip transmission lines. Also,

attempts should be made to describe the dispersive behaviour of coupled microstrip transmission lines and lines having discontinuties such as bends, open and short circuits. Finally, by incorporating the material presented in this thesis with the results of future work, an attempt could be made to design precision microstrip components and solid state microwave oscillator circuits, which at the present time are often designed using a trial and error method.

APPENDIX A

MEASUREMENT OF Q

The quality factor, Q is defined as[24,25]

$$Q = 2\pi \frac{\text{Total energy stored}}{\text{Energy Dissipated per cycle}} \qquad \text{A.1}$$

$$= \omega \frac{U}{P} \qquad \text{A.2}$$

where ω is the angular frequency, U is the total energy stored and P is the total power lost. The loaded quality factor, Q_L, of the cavity is given by[7,24]

$$\frac{1}{Q_L} = \frac{1}{Q_o} + \frac{1}{Q_{ext}} + \frac{1}{Q_{rad}} \qquad \text{A.3}$$

where

Q_o = unloaded quality factor of the cavity and is determined by the dissipation in the cavity.

Q_{ext} = external quality factor and is determined by the coupling system.

Q_{rad} = radiation quality factor and is determined by the radiation losses of the cavity and the coupling system.

The equivalent circuit of a transmission cavity (resonant ring structure[3]) with coupling elements is shown in Figure A.1. The

coupling between the cavity and the transmission lines (coupling probes) is represented by both resistive and reactive components. The inductance L_1 and L_2 in the equivalent circuit represent the self inductances of the coupling elements which are due to the fringing field caused by the discontinuity at the junction of the transmission line and the cavity. The losses (dissipative and radiative) of the coupling structure are represented by R_{S1} and R_{S2}. The dissipative losses of the cavity are represented by R_c while the radiative losses are represented by the resistance R_r. The equivalent circuit is simplified for analysis by referring to source and load impedances to the cavity circuit as shown in Figure A.1C. The loaded quality factor of the system is given by[24]

$$Q_L = \frac{\omega_o L}{R_c + R_r + \frac{(\omega M_1)^2}{Z'_o} + \frac{(\omega M_2)^2}{Z'_o}} \qquad A.4$$

where

$$Z'_o = \frac{Z_o R_S}{Z_o + R_S}$$

Z_o = characteristic impedance of the input and output coupling probes.

The input and output coupling coefficients are defined as[24]

$$\beta_1 = \frac{(\omega M_1)^2}{Z'_o R_c} =$$ ratio of the coupled resistance at the input part of the cavity to the cavity resistance R_c

$$\beta_2 = \frac{(\omega M_2)^2}{R_c Z_o'} = \text{ratio of the coupled resistance at the output part of the cavity to the cavity resistance } R_c.$$

Therefore

$$Q_L = \frac{Q_o}{1 + \frac{R_r}{R_c} + \beta_1 + \beta_2} \qquad \text{A.5}$$

where

$$Q_o = \frac{\omega_o L}{R_c} \text{ by definition} \qquad \text{A.6}$$

from A.3 and A.6

$$Q_{ext} = \frac{Q_o}{\beta_1 + \beta_2} \qquad \text{A.7}$$

$$Q_{rad} = \frac{Q_o}{(R_r/R_c)} \qquad \text{A.8}$$

As the coupling gap width between the probes and the cavity is increased:

(i) Losses represented by R_c remain constant and so Q_o remains constant as well (see Figure A.2).

(ii) The coupling coefficients decrease and approach zero for large gaps and so Q_{ext} increases asymptotically to infinity (see Figure A.2)

(iii) The radiation losses increase and so Q_{rad} decreases. (*It has been observed experimentally that approximately 20% of the incident power is radiated from an open circuited microstrip transmission line while Lewin*[11] *has shown that a much smaller fraction of power is radiated (of the order of 4%) from a short circuited transmission line. Increasing the gap width from a small value to a large value may be considered (to a first approximation) to correspond to changing the transmission line termination from a 'short circuit' to an 'open circuit' condition. Therefore the variation of* Q_{rad} *shown in Figure A.2 is expected).*

While no attempt was made to mathematically describe Q_L as a function of gap width, it was experimentally verified (see Figure 11) that Q_L varies in the fashion shown in Figure A.2.

APPENDIX B

SURFACE WAVE SOLUTIONS FOR A DIELECTRIC SLAB

ON A CONDUCTING PLANE

Transverse surface waves of both the even TM and odd TE type may be guided along a dielectric sheet or slab on a conducting plane[28]*. The TM modes have a single component of magnetic field H_x and electric field components E_y and E_z (see Figure 17) while TE modes have components E_x, H_y and H_z. The waves propagate in the z direction with a propagation constant β, which is to be determined. Solutions for TM and TE modes are found by solving the wave equation in the dielectric and in the air with proper boundary conditions at the interface (fields decay with distance from the air dielectric interface for both type of modes[28]).

B.1 TM Surface Wave Solutions

A solution for TM surface wave modes having $H_z = 0$ and $\frac{\partial}{\partial x} = 0$ (i.e. no variation with respect to the x axis) is developed below.

The cut off wave number, K_c, is denoted by p_d in the dielectric region and by jp_a in the air region ($y > h$, where it is assumed that the fields decay exponentially with distance for the air dielectric interface) writing the wave equation for E_z:

* Odd TM and even TE modes are not possible since the tangential electric field component does not vanish on the conducting plane.

$$\nabla_{xy}^2 E_z + K_c^2 E_z = 0 \qquad \text{B.1}$$

where

$$\nabla_{xy}^2 = \frac{\partial^2}{\partial x^2} + \frac{\partial^2}{\partial y^2} = \frac{\partial^2}{\partial y^2} \left(\text{since } \frac{\partial}{\partial x} = 0\right) \qquad \text{B.2}$$

we have

$$\frac{\partial^2 Ez}{\partial y^2} + p_d^2 Ez = 0, \quad 0 < y < h \qquad \text{B.3}$$

$$\frac{\partial^2 Ez}{\partial y^2} - p_a^2 Ez = 0, \quad y > h \qquad \text{B.4}$$

Since the cut off wave number $K_c^2 = w^2\mu\varepsilon - \beta_{TM}^2$, K_c must be different in the two regions (air and dielectric, $w^2\mu\varepsilon$ being dependent on the medium). Solutions for equations B.3 and B.4 in the dielectric and air regions, such that Ez = 0 on the conductor (y = 0) and at $y = \infty$, are given respectively by:

$$Ez = A \sin p_d y \qquad 0 < y < h \qquad \text{B.5}$$

$$E = B e^{-p_a y} \qquad y > h \qquad \text{B.6}$$

where A and B are constants. At the air dielectric interface (y = h), the tangential components of both the electric and magnetic fields must be continuous for all values of z. Therefore the propagation

constant β_{TM} of the TM surface wave modes must be equal in both the regions, i.e.:

$$\beta_{TM}^2 = \varepsilon_r \beta_a^2 - p_d^2 = \beta_a^2 + p_a^2 \qquad \text{B.7}$$

or

$$p_d^2 + p_a^2 = (\varepsilon_r - 1)\, \beta_a^2 \qquad \text{B.8}$$

Also from equations B.5 and B.6 (E_z is continuous at y = h), we have

$$A \sin p_d h = B\, e^{-p_a h} \qquad \text{B.9}$$

The three unknown $\frac{A}{B}$, p_d and p_a in the above equations (B.8 and B.9) can be determined from the requirement that H_x be continuous at y = h. This gives the following equation in terms of E_z:

$$\frac{\varepsilon_r}{p_d^2} \frac{\partial E_z}{\partial y} \bigg|_{y=h-} = -\frac{1}{p_a^2} \frac{\partial E_z}{\partial y} \bigg|_{y=h+} \qquad \text{B.10}$$

From equations B.5, B.6 and B.10, we have

$$\frac{\varepsilon_r A}{p_d} \cos p_d h = \frac{B}{p_a} e^{-p_a h} \qquad \text{B.11}$$

Dividing equation B.9 by equation B.11 and multiplying both sides by h, we have

$$\varepsilon_r p_a h = p_d h \tan p_d h \qquad \text{B.12}$$

If a solution for p_a real exists, the solution is for a surface wave, since the fields decay exponentially in the y direction and propagate in the z direction.

Equations B.8 and B.12 may now be solved for p_a and p_d. Since p_a and p_d can not be solved directly, they are determined graphically. For this purpose it is convenient to rewrite equations B.8 and B.12 as follows:

$$(p_a h)^2 + (p_d h)^2 = (\varepsilon_r - 1)(\beta_a h)^2 \qquad \text{B.13}$$

and

$$\varepsilon_r p_a h = p_d h \tan p_d h \qquad \text{B.14}$$

At a given frequency, equation B.13 is a circle of radius $(\varepsilon_r - 1)^{\frac{1}{2}} \beta_a h$ in the $p_d h$, $p_a h$ plane. Equation B.14 is plotted in the same plane. The point of intersection between the two curves determine the eigen values p_a and p_d at that frequency (see Figures 19 to 23).

Since p_a must be real and positive (for exponentially decaying waves in the y direction) for a surface wave mode, only those points of intersections that lie in the interval $n\pi < p_d h < n\pi + \frac{\pi}{2}$, (where n is an even integer for even modes) correspond to a surface wave solution[28]. The first even TM mode corresponds to n = 0 and is called the TM_o surface wave mode. It will be shown later that the TM_o mode have zero low frequency cut off, while higher order even TM modes have finite lower cut off frequencies depending on the order of the mode.

B.2 TE Surface Wave Solutions

The solutions for the TE modes are found in a manner similar to that for the TM modes. The eigen value equations for the odd TE modes are[30]

$$(p_a h)^2 + (p_d h)^2 = (\varepsilon_r - 1)(\beta_a h)^2 \qquad \text{B.15}$$

and

$$\varepsilon_r p_a h = -p_d h \cot p_d h \qquad \text{B.16}$$

where only those points of intersection that occur in the interval $n\pi - \frac{\pi}{2} \leq p_d h \leq n\pi$ (where n is any odd integer) correspond to an odd TE surface wave solution. The lowest order TE mode is the TE_1 mode which exists in the interval $\frac{\pi}{2} \leq p_d h \leq \pi$.

B.3 Lower Cut Off Frequency of TM and TE Surface Wave Modes

The cut off condition for even TM and TE modes is given by

$$p_d h = \frac{n\pi}{2} \qquad \text{B.17}$$

where n = 0, 2, 4 .... (even TM modes) and n = 1,3, 5 .... (odd TE modes). For $p_d h = \frac{n\pi}{2}$, the equations B.14 and B.16 give

$$p_a = 0$$

Therefore equations B.13 and B.15 give

$$p_d h = (\varepsilon_r - 1)^{\frac{1}{2}} \beta_{co}$$

$$= (\varepsilon_r - 1)^{\frac{1}{2}} \frac{2\pi f_{co}}{c} \qquad \text{B.18}$$

where the subscript co represents cut off.

Equating B.17 and B.18 we have

$$f_{co} = \frac{nc}{4h(\varepsilon_r - 1)^{\frac{1}{2}}} \qquad \text{B.19}$$

Equation B.19 gives the low frequency cut off for even TM modes (n even) and odd TE modes (n odd). This equation shows that in the frequency interval, $0 < f < \frac{c}{4h(\varepsilon_r - 1)^{\frac{1}{2}}}$, only the TM_o mode exists.

B.4 The Effective Dielectric Constant and Phase Velocity of the TM_o Mode

The effective dielectric constant of the TM_o mode is given by

$$\varepsilon_{eff_{TM_o}} = \left(\frac{\beta_{TM_o}}{\beta_a} \right)^2 \qquad \text{B.20}$$

and is determined by substituting the value of p_a or p_d in equation B.7.

The phase velocity of the TM_o mode is given by

$$\left(V_{ph} \right)_{TM_o} = \frac{c}{(\varepsilon_{eff_{TM_o}})^{\frac{1}{2}}}$$

$$= \frac{\beta_a c}{\beta_{TM_o}} \qquad \text{B.21}$$

Using equation B.7, we get

$$\left(V_{ph} \right)_{TM_o} = \frac{\beta_a c}{(\beta_a^2 + p_a^2)} = \frac{\beta_a c}{(\varepsilon_r \beta_a^2 - p_d^2)^{\frac{1}{2}}} \qquad \text{B.22}$$

At zero frequency $p_a = 0$ and $(V_{ph})_{TM_o}$ is equal to the velocity of light in air. As the frequency is increased, p_a increases and so the phase velocity decreases. For this reason a surface wave is called a slow wave. At very high frequencies $\varepsilon_r \beta_a^2 >> p_d^2$, and therefore the phase velocity is given by

$$\left(V_{ph} \right)_{TM_o} \approx \frac{\beta_a c}{\beta_a \varepsilon_r^{\frac{1}{2}}} = \frac{c}{\varepsilon_r^{\frac{1}{2}}} \qquad \text{B.23}$$

which is the velocity of light in the dielectric region. A typical variation of the phase velocity of the TM_o waves with frequency is shown in Figure B.1.

APPENDIX C

COUPLED MODE THEORY

C.1 General Formalism

A total of S equations are required to describe the coupling of modes waveguiding into a system in which S modes are present. The transmission line equations for a set of coupled transmission modes may be written in the form[29]:

$$j \frac{\partial a_r}{\partial z} - \sum_S \beta_{rS} a_S = 0 \qquad C.1$$

where

a_r = amplitude of the rth mode

a_S = amplitude of the Sth mode

β_{rS} = coupling coefficient between the rth mode and the Sth mode

β_{rr} = uncoupled propagation constant of the rth mode

This set of S equations may also be written in matrix form:

$$j \frac{\partial \bar{a}}{\partial z} - \bar{\beta}\,\bar{a} = 0 \qquad C.2$$

where

$$\bar{a} = \begin{bmatrix} a_1 \\ a_2 \\ \cdot \\ \cdot \\ \cdot \\ a_r \\ \cdot \\ \cdot \\ \cdot \\ a_n \end{bmatrix} \qquad \bar{\beta} = \begin{bmatrix} \beta_{11} & \beta_{12} \cdots\cdots \beta_{1n} \\ \beta_{21} & \beta_{22} \cdots\cdots \beta_{2n} \\ \cdot & \\ \cdot & \\ \cdot & \\ \beta_{r1} & \beta_{r2} \cdots\cdots \beta_{rn} \\ \cdot & \\ \cdot & \\ \cdot & \\ \beta_{n1} & \beta_{n2} \cdots\cdots \beta_{nn} \end{bmatrix} \qquad \text{C.3}$$

Solutions to equation C.2 are desired in the form:

$$\bar{a}(z) = \bar{A}\, e^{-j\beta z} \qquad \text{C.4}$$

where $\bar{A}$ is a constant column matrix with components A_r. The $\bar{\beta}$ values which may be determined describe the waves propagating in the coupled system. Combining equation C.4 with equation C.2, the problem reduces to an eigen value problem,

$$\beta \bar{a} - \bar{\beta} \bar{a} = 0 \qquad \text{C.5}$$

where the eigen values are β_i and the eigen functions are a_i. The eigen values β_i are the propagation constants of the coupled system. The general solution of C.1 consists of a summation over all the allowed

eigen functions:

$$a(z) = \sum_i A^i e^{-j\beta_i z} \qquad C.6$$

C.2 Coupling of Two Waves

For two modes (i.e. S=2), equation C.2 gives

$$j \frac{\partial a_1}{\partial z} - \beta_{11} a_1 - \beta_{12} a_2 = 0 \qquad C.7$$

$$j \frac{\partial a_2}{\partial z} - \beta_{21} a_1 - \beta_{22} a_2 = 0 \qquad C.8$$

The eigen values, β_i, are found from equation C.5, so we have

$$\beta a_1 = \beta_{11} a_1 + \beta_{12} a_2 \qquad C.9$$

$$\beta a_2 = \beta_{21} a_1 + \beta_{22} a_2 \qquad C.10$$

Combining equations C.9 and C.10, we have

$$a_1 [\beta^2 - \beta(\beta_{11} + \beta_{22}) + \beta_{11} \beta_{22} + \beta_{12}\beta_{21}] = 0 \qquad C.11$$

since $a_1 \neq 0$, we may write

$$\beta^2 - \beta(\beta_{11} + \beta_{22}) + \beta_{11} \beta_{22} + \beta_{12} \beta_{21} = 0 \qquad C.12$$

which gives two solutions of β for the two coupled modes:

$$\beta_{1,2} = \frac{\beta_{11} + \beta_{22}}{2} \pm \sqrt{\left(\frac{\beta_{11} - \beta_{22}}{2}\right)^2 + \beta_{12}\,\beta_{21}} \qquad \text{C.13}$$

where β_{11}, β_{22}, β_{12} and β_{21} have the units of radians/cm.

Equation C.13 may be applied to describe the coupling between the TEM and TM_o modes in a microstrip transmission line. This equation is rewritten in the following form:

$$\varepsilon_{eff_{1,2}} = \left[\frac{\sqrt{\varepsilon_{eff_o}} + \sqrt{\varepsilon_{eff_{TM_o}}}}{2} \pm \sqrt{\left(\frac{\varepsilon_{12}}{\xi}\right)\left(\frac{\varepsilon_{21}}{\xi}\right)\xi^2 + \left(\frac{\sqrt{\varepsilon_{eff_o}} - \sqrt{\varepsilon_{eff_{TM_o}}}}{2}\right)^2} \right]^2 \qquad \text{C.14}$$

where ε_{eff} is the effective dielectric constant and is defined as

$$\varepsilon_{eff} = \left(\frac{\beta}{\beta_a}\right)^2 \qquad \text{C.15}$$

Reciprocity is satisfied for the system considered in this thesis and therefore

$$\varepsilon_{12} = \frac{\beta_{12}}{\beta_a} = \frac{\beta_{21}}{\beta_a} = \varepsilon_{21}$$

The coupling coefficient between the two modes is given by

$$\frac{\varepsilon_{12}}{\xi} = \frac{\varepsilon_{21}}{\xi}$$

where

$$\xi^2 = \left(\varepsilon_{eff_o}\, \varepsilon_{eff_{TM_o}}\right)^{\frac{1}{2}}$$

The effective dielectric constant of the dispersive microstrip is given by ε_{eff_1} (Mode 1, + sign) and ε_{eff_2} (Mode 2, - sign), while the effective dielectric constant for the TM_o mode is given by $\varepsilon_{eff_{TM_o}}$. Equation C.13 may be solved for ε_{12}^2 :

$$\varepsilon_{12}^2 = \left[\sqrt{\varepsilon_{eff_1}} - \frac{\sqrt{\varepsilon_{eff_o}} + \sqrt{\varepsilon_{eff_{TM_o}}}}{2}\right]^2 - \left[\frac{\sqrt{\varepsilon_{eff_o}} - \sqrt{\varepsilon_{eff_{TM_o}}}}{2}\right]^2$$

C.16

where only ε_{eff_1} is considered, since only Mode 1 exists in the range of frequencies of interest.

APPENDIX D

UPPER FREQUENCY LIMIT f_ℓ

It has been shown (Appendix B) that for a dielectric of thickness h on a conducting plane, the solution for the TM_o surface wave mode may be determined graphically from the following equations:

$$\varepsilon_r p_a = p_d \tan p_d h \qquad \text{D.1}$$

$$p_a^2 + p_d^2 = (\varepsilon_r - 1)\,\beta_a^2 \qquad \text{D.2}$$

where

p_a = transverse wave number of the TM_o mode in the air region

p_d = transverse wave number of the TM_o mode in the dielectric region

β_a = free space wave number = $\frac{2\pi f}{c}$

and

$$\varepsilon_{eff_{TM_o}} = 1 + \frac{p_a^2}{\beta_a^2} \qquad \text{D.3}$$

The static effective dielectric constant of a microstrip transmission line can be calculated (with an accuracy of $\pm$ 2%) from the equation[10]:

$$\varepsilon_{eff_o} = \frac{\varepsilon_r+1}{2} + \frac{\varepsilon_r-1}{2}\left(1 + 10\,\frac{h}{w}\right)^{-\frac{1}{2}} \qquad \text{D.4}$$

which, for $\frac{w}{h} << 1$ reduces to

$$\varepsilon_{eff_o} = \frac{\varepsilon_r+1}{2} \qquad \text{D.5}$$

The phase velocity of the TM_o surface wave decreases with increasing frequency (see Figure B.1). The coupling between the TM_o surface wave mode and the TEM mode may be assumed to be strong when both modes have phase velocities of the same order. Thus equating D.3 and D.4, we have

$$\frac{p_a^2}{\beta_\ell^2} = \frac{\varepsilon_r-1}{2}\left[1 + \left(1 + 10\,\frac{h}{w}\right)^{-\frac{1}{2}}\right] \qquad \text{D.6}$$

where β_ℓ is the free space wave number $= \frac{2\pi f_\ell}{c}$ at a frequency f_ℓ, at which

$$\varepsilon_{eff_o} = \varepsilon_{eff_{TM_o}}$$

Substituting equation D.6 in D.2, we have

$$p_d^2 = \frac{\varepsilon_r-1}{2}\left[1 - \left(1 + 10\,\frac{h}{w}\right)^{\frac{1}{2}}\right]\left[\frac{2\pi f_\ell}{c}\right]^2 \qquad \text{D.7}$$

Equation D.1 gives

$$p_d h = \arctan \varepsilon_r \frac{p_a}{p_d} \qquad D.8$$

Substituting the value of p_a and p_d from equations D.6 and D.7 in Equation D.8, we have

$$\left[\frac{\varepsilon_r - 1}{2}\right]^{\frac{1}{2}} \left[1 - \left(1 + 10\frac{h}{w}\right)^{-\frac{1}{2}}\right]^{\frac{1}{2}} \left[\frac{2\pi f_\ell}{c}\right] h = \arctan \varepsilon_r \left[\frac{1 + \left(1 + 10\frac{h}{w}\right)^{-\frac{1}{2}}}{1 - \left(1 + 10\frac{h}{w}\right)^{-\frac{1}{2}}}\right]^{\frac{1}{2}}$$

or

$$f_\ell = \frac{c}{2\pi h}\left(\frac{2}{\varepsilon_r - 1}\right)^{\frac{1}{2}} \left[1 - \left(1 + 10\frac{h}{w}\right)^{-\frac{1}{2}}\right]^{-\frac{1}{2}} \arctan \varepsilon_r \left[\frac{1 + \left(1 + 10\frac{h}{w}\right)^{-\frac{1}{2}}}{1 - \left(1 + 10\frac{h}{w}\right)^{-\frac{1}{2}}}\right]^{\frac{1}{2}}$$

D.8

which, for $\frac{w}{h} \ll 1$, reduces to[20]

$$f_\ell = \frac{c}{2\pi h}\sqrt{\frac{2}{\varepsilon_r - 1}} \arctan \varepsilon_r \qquad D.9$$

APPENDIX E

DETERMINATIONS OF THE CONSTANTS n_2, n_3 and K

(A) Determination of n_2

For a microstrip transmission line one can find the effective dielectric constant experimentally. For a fixed ε_r, h and $\frac{w'}{h}$, we choose the experimental values of ε_{eff_1} at frequencies, f_1, f_2, f_3,...,f_m, ..., f_N. Then from equation 3.11 we have:

$$\frac{X(f_m)}{X(f_{m-1})} = \left[\frac{f_m}{f_{m-1}}\right]^{n_2} \quad \text{where } m = 2,3,\ldots, N$$

i.e.

$$n_2 = \frac{\log\left\{X(f_m)/X(f_{m-1})\right\}}{\log (f_m/f_{m-1})}$$

a value of n_2 may be found for each of the N-1 equations. The average value of n_2 then is given by

$$n_2 = \frac{1}{N-1} \sum_{m=2}^{m=N} \frac{\log\left\{X(f_m)/X(f_{m-1})\right\}}{\log (f_m/f_{m-1})} \qquad \text{E.1}$$

(B) Determination of n_3

Having found n_2 we now choose the experimental value of ε_{eff_1} for microstrip transmission lines having different values of $\frac{w}{h}$ ratios, ε_r and h being same for all the lines. Then at a given frequency and for $\frac{w'}{h} = x$ and $\frac{w'}{h} = y$, we have from equation 3.11:

$$n_3 = \frac{\log \left\{X(f_m)\cdot(f_\ell)^{n_2}\right\}_{\frac{w'}{h}=x} - \log \left\{X(f_m)\cdot(f_\ell)^{n_2}\right\}_{\frac{w'}{h}=y}}{\log \left(\frac{x}{y}\right)}$$

Thus the average value of n_3 is given by

$$n_3 = \frac{1}{N} \sum_{m=1}^{N} \frac{\log \left\{X(f_m)\cdot(f_\ell)^{n_2}\right\}_{\frac{w'}{h}=x} - \log \left\{X(f_m)\cdot(f_\ell)^{n_2}\right\}_{\frac{w'}{h}=y}}{\log \left(\frac{x}{y}\right)} \qquad \text{E.2}$$

Having determined n_2 and n_3, K can be directly calculated from equation 3.11, where $X(f_m)$ is known from experimental results. Thus the average value of K is given by

$$k = \frac{1}{N} \sum_{m=1}^{N} \frac{X(f_m)}{(\eta-1)^2 \left[\frac{w'}{h}\right]^{n_3} \left[\frac{f_m}{f_\ell}\right]^{n_2}} \qquad \text{E.3}$$

where the frequencies f_1 to f_N may not necessarily be the same.

The average values of n_2, n_3 and k, calculated using equations

E.1 to E.3 and the experimental dispersion data, were found to be $\frac{4}{3}$, $\frac{3}{4}$ and 0.22 respectively.

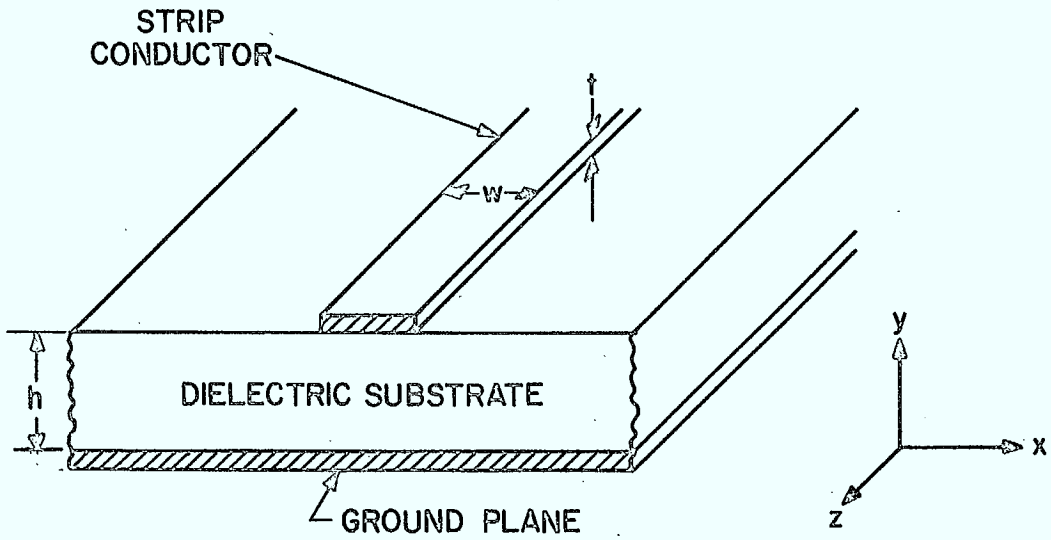

h=SUBSTRATE THICKNESS
t="STRIP" CONDUCTOR
w="STRIP" CONDUCTOR WIDTH

FIG. 1 —MICROSTRIP TRANSMISSION LINE.

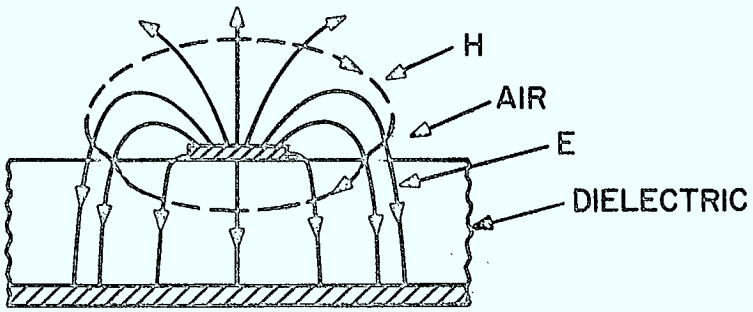

FIG. 2-ELECTRIC AND MAGNETIC FIELDS IN THE VICINITY OF A MICROSTRIP.

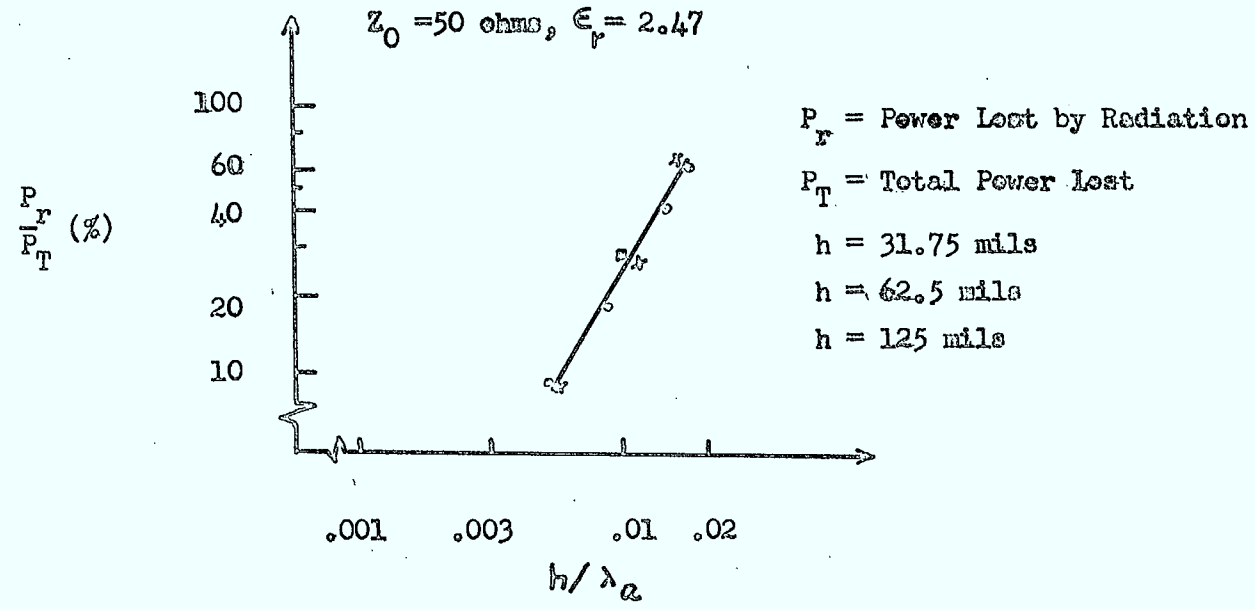

FIG. 3 POWER RADIATED VS. NORMALISED SUBSTRATE THICKNESS FOR A TRANSMISSION LINE RESONATOR[12].

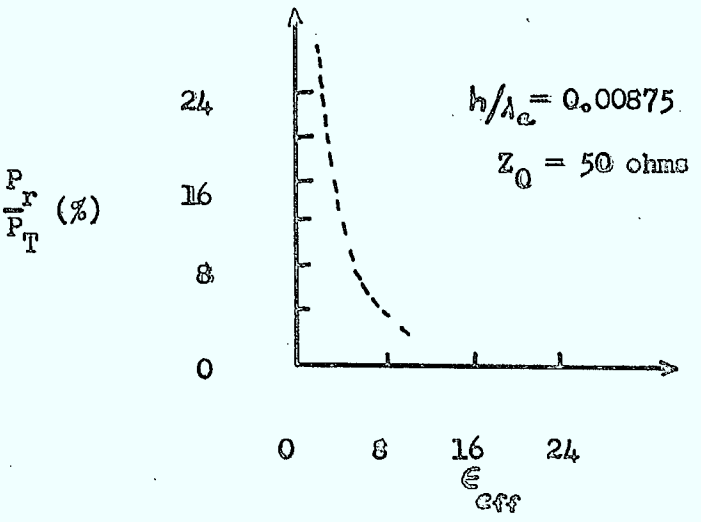

FIG. 4 POWER RADIATED VS. SUBSTRATE EFFECTIVE DIELECTRIC CONSTANT FOR A TRANSMISSION LINE RESONATOR[12].

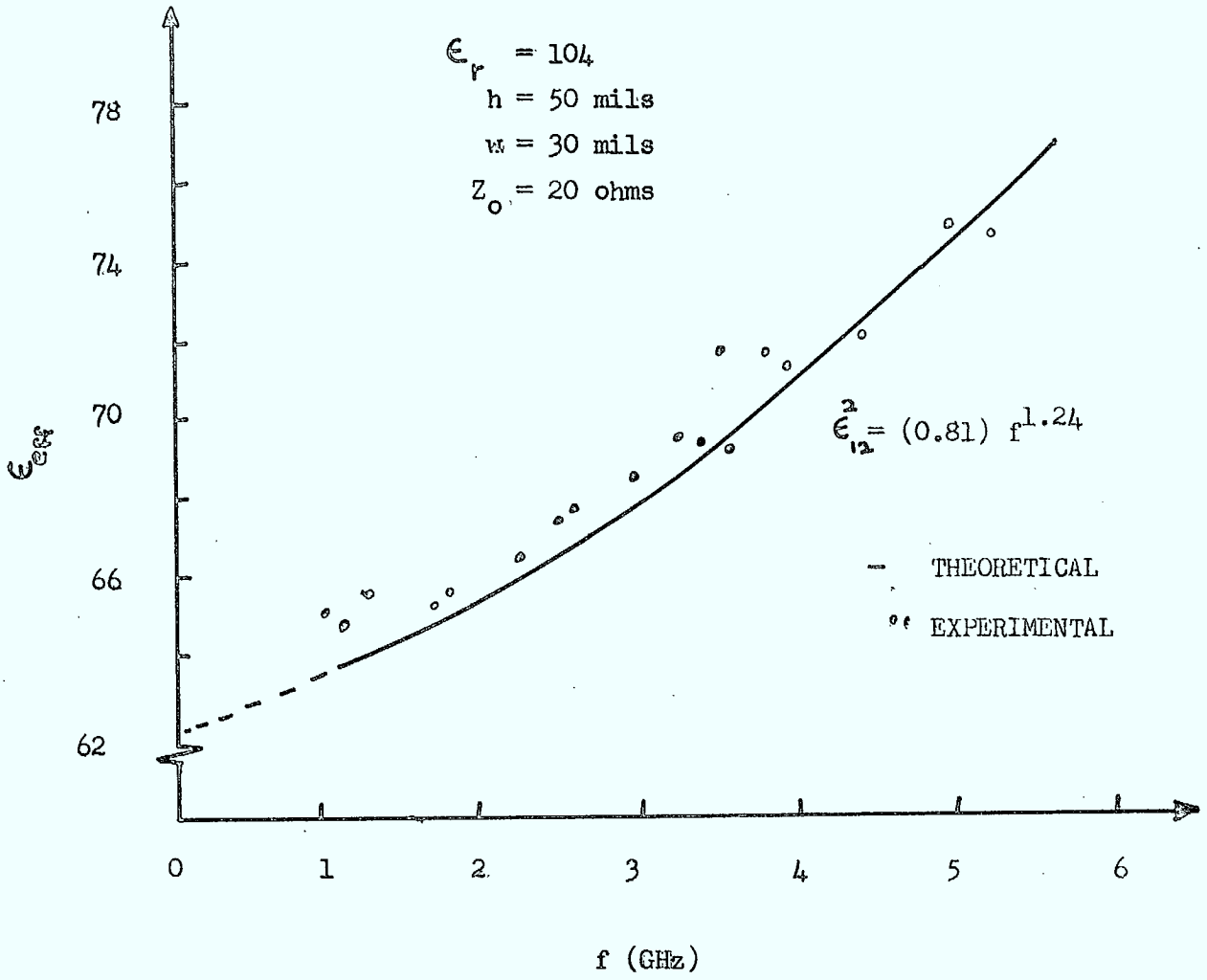

FIG. 5 EFFECTIVE DIELECTRIC CONSTANT VS. FREQUENCY FOR A RUTILE MICROSTRIP[1]

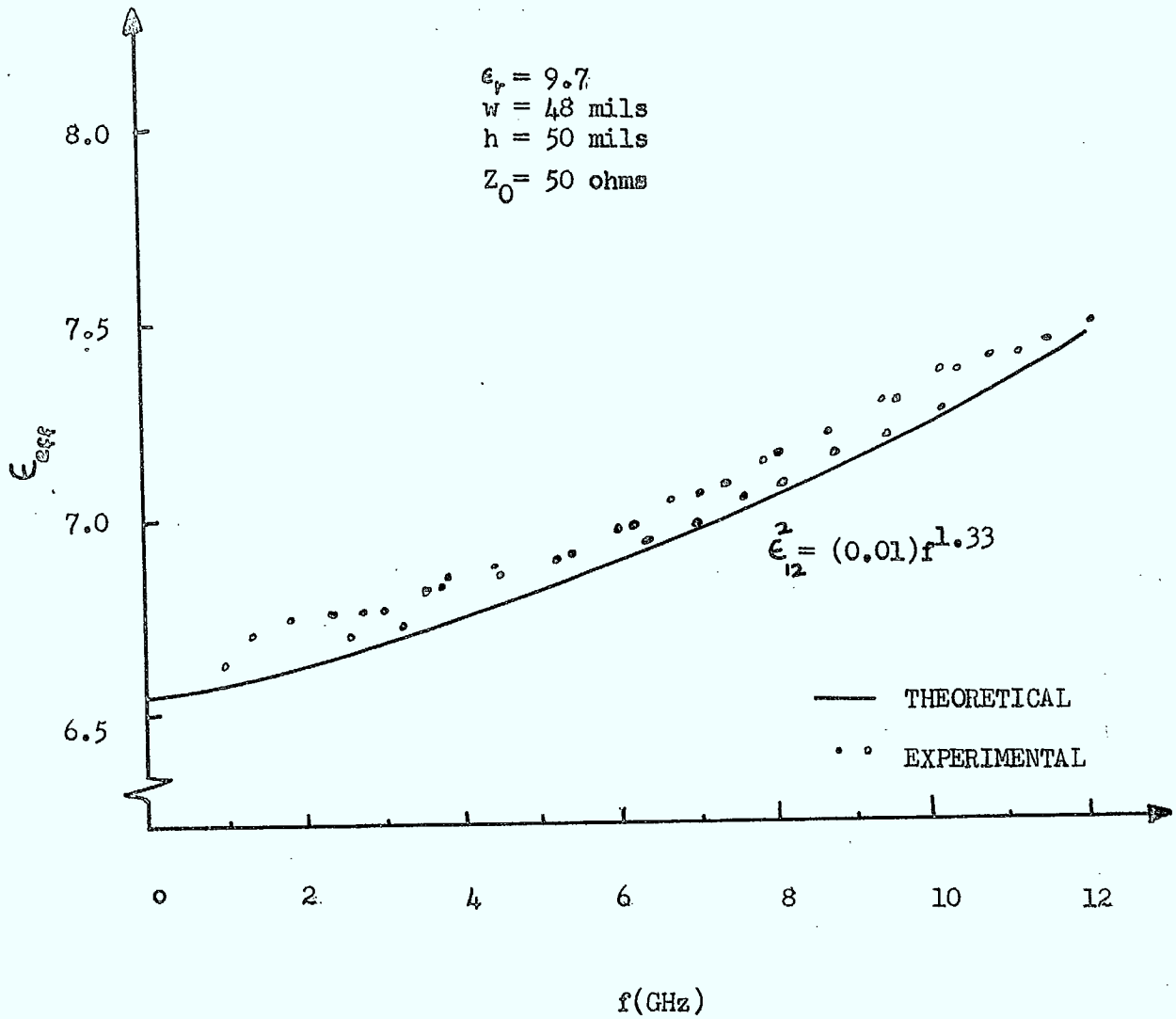

FIG. 6 EFFECTIVE DIELECTRIC CONSTANT VS. FREQUENCY FOR AN ALUMINA MICROSTRIP[1].

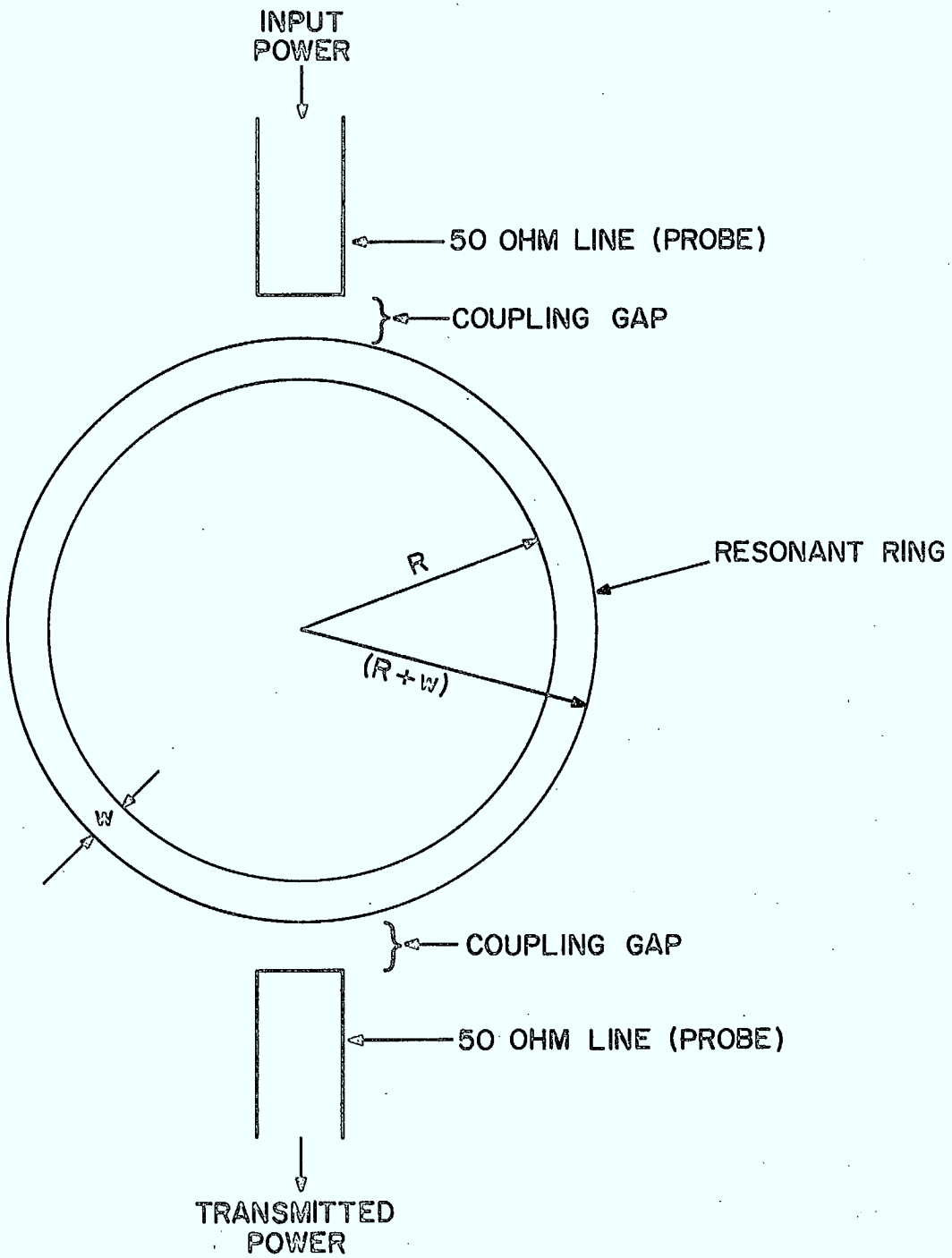

FIG. 7 RESONANT RING FOR THE MEASUREMENT OF ϵ_{eff}.

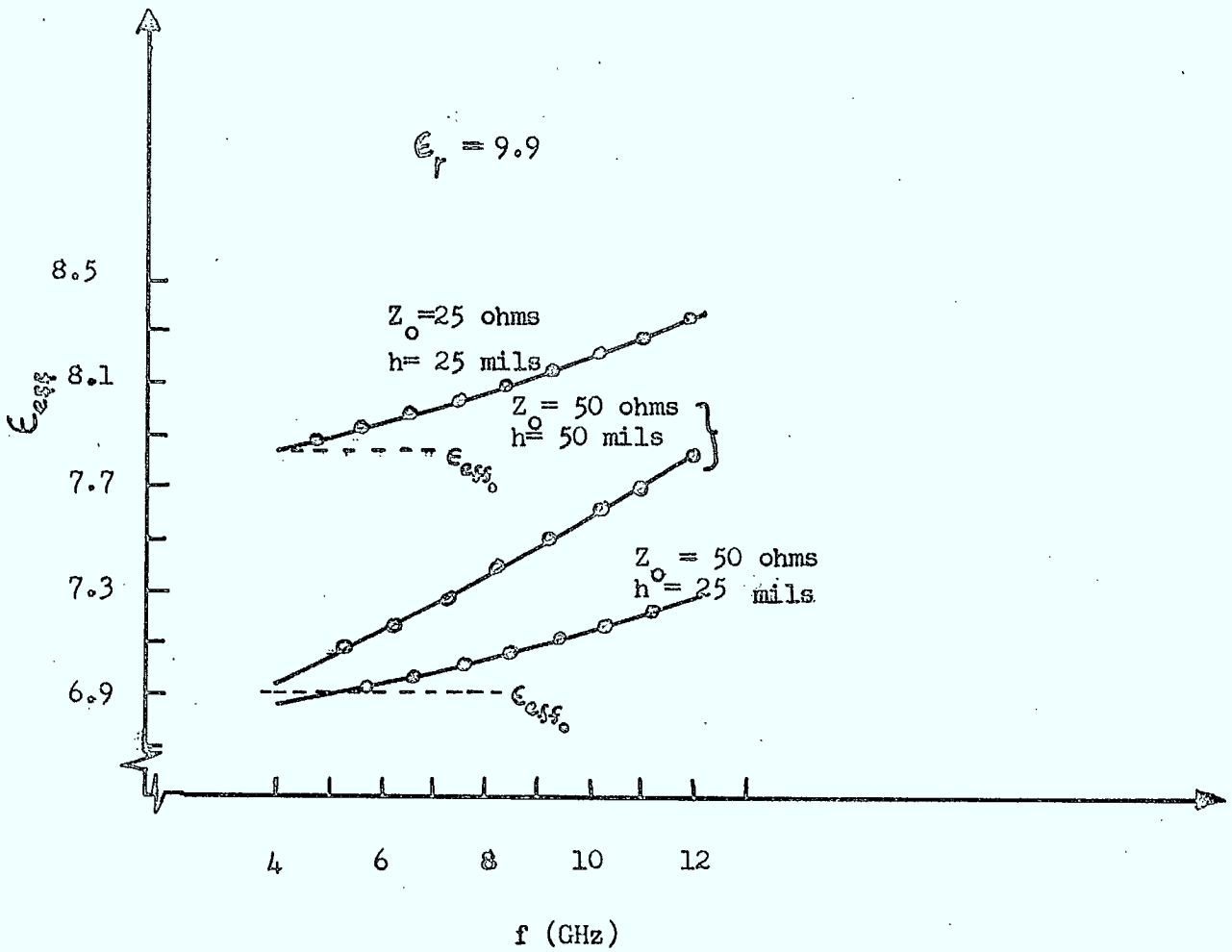

FIG. 8 EFFECTIVE DIELECTRIC CONSTANT VS. FREQUENCY FOR AN ALUMINA MICROSTRIP[2].

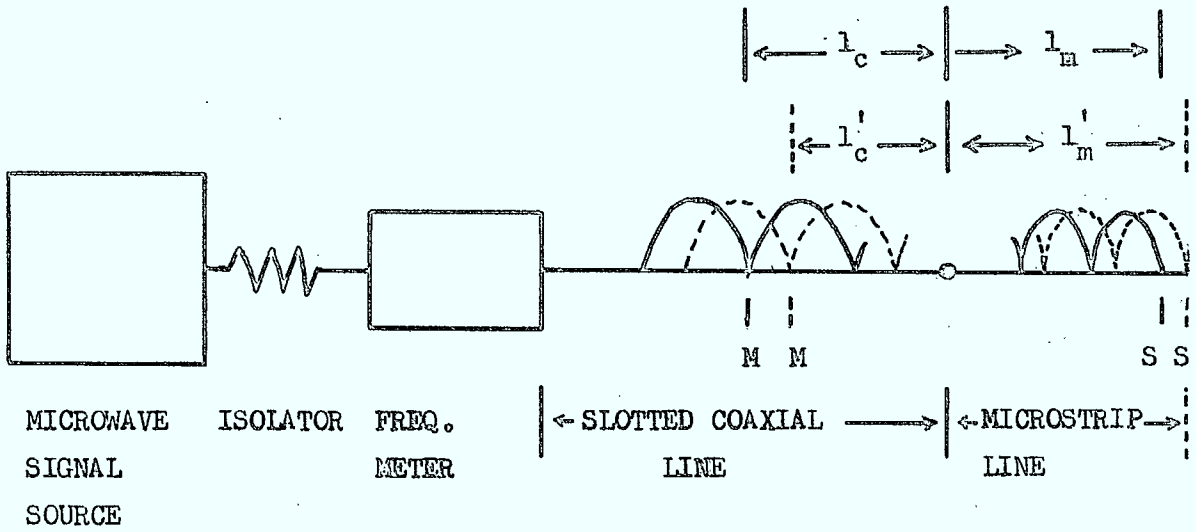

——— INITIAL POSITION

— — FINAL POSITION

S MICROSTRIP SHORT

M VOLTAGE MINIMA

FIG. 9 WAVE LENGTH MEASUREMENT USING A SLOTTED LINE.
(STANDING WAVE DETECTION METHOD)

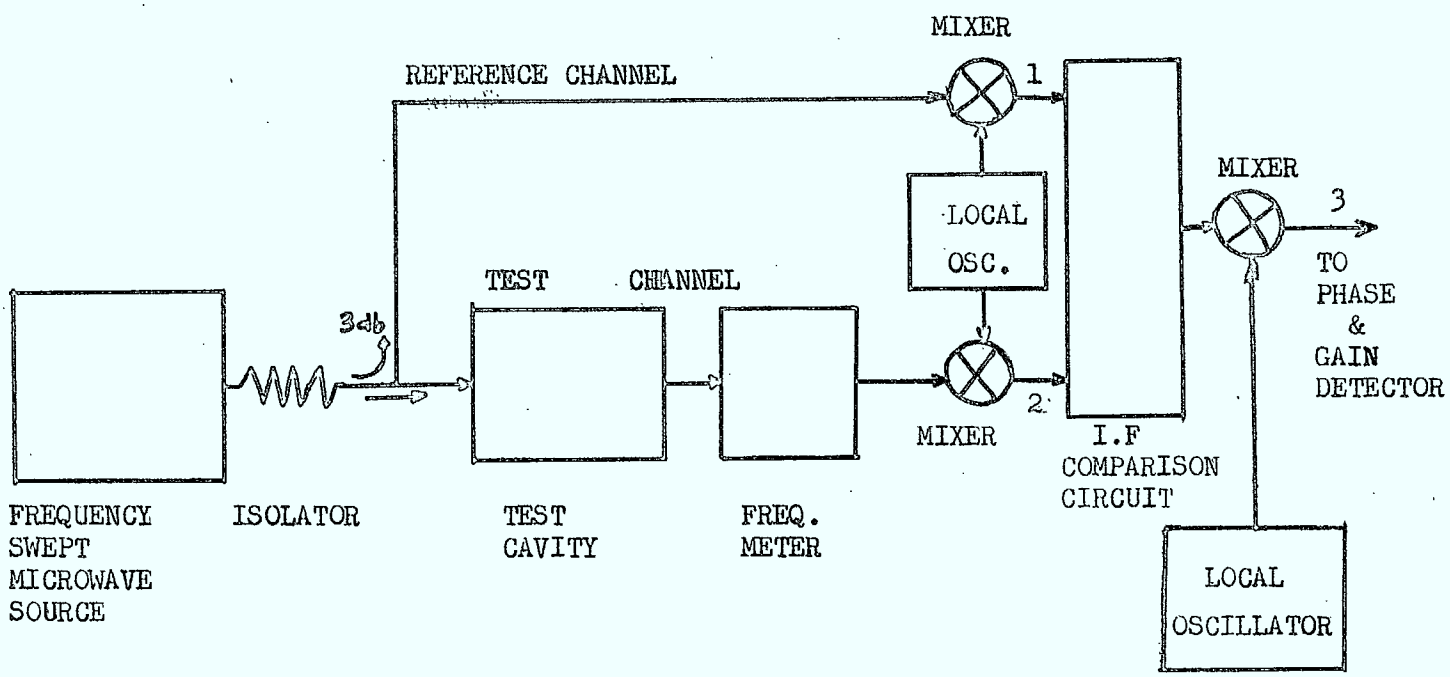

1 & 2 20 MHz IF

3 278 KHz IF

FIG. 10 MICROWAVE BRIDGE FOR TRANSMISSION MEASUREMENT.

(RESONANCE METHOD)

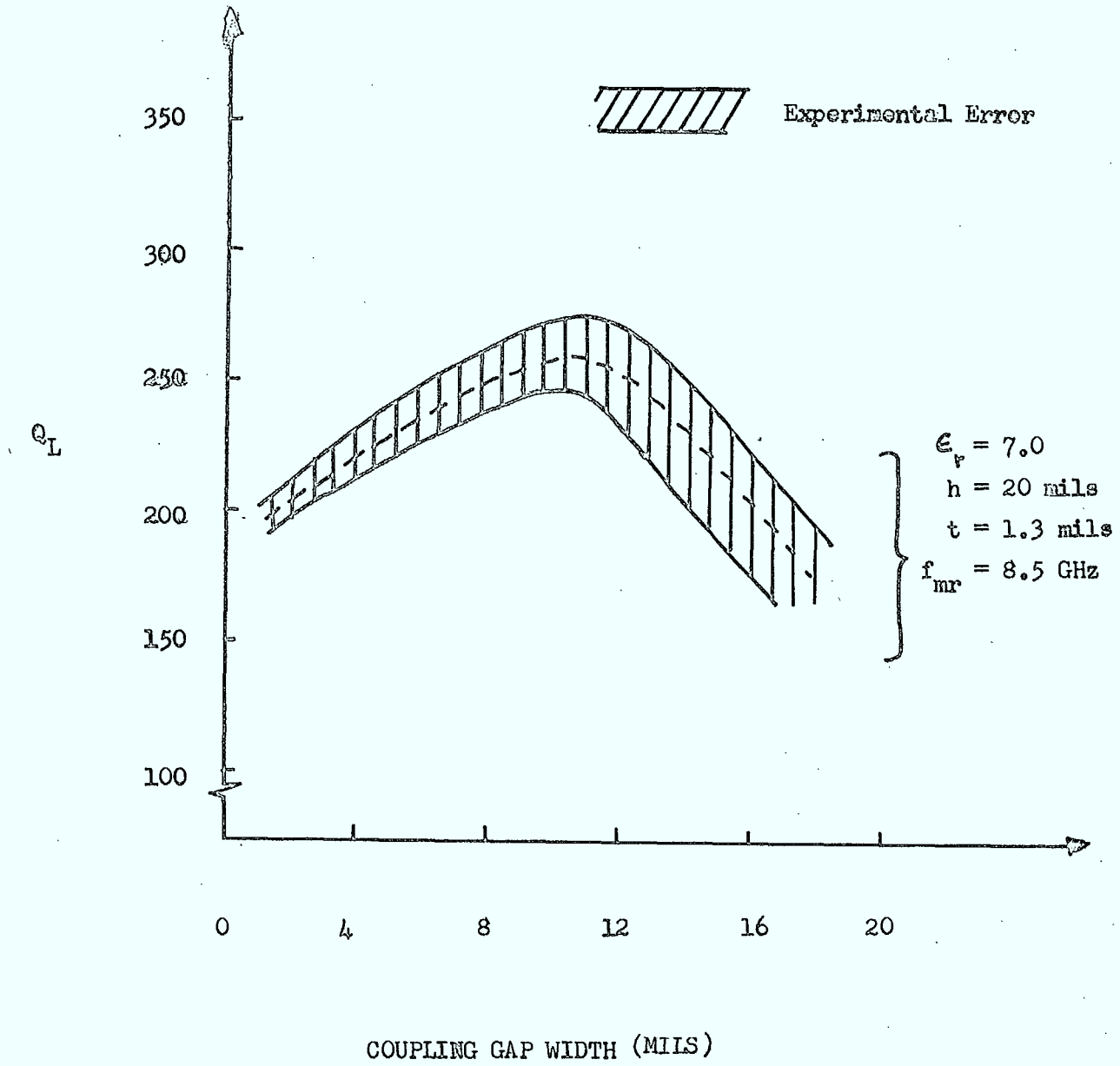

FIG. 11 VARIATION OF Q_L OF THE RING RESONATOR VS. COUPLING GAP WIDTH.

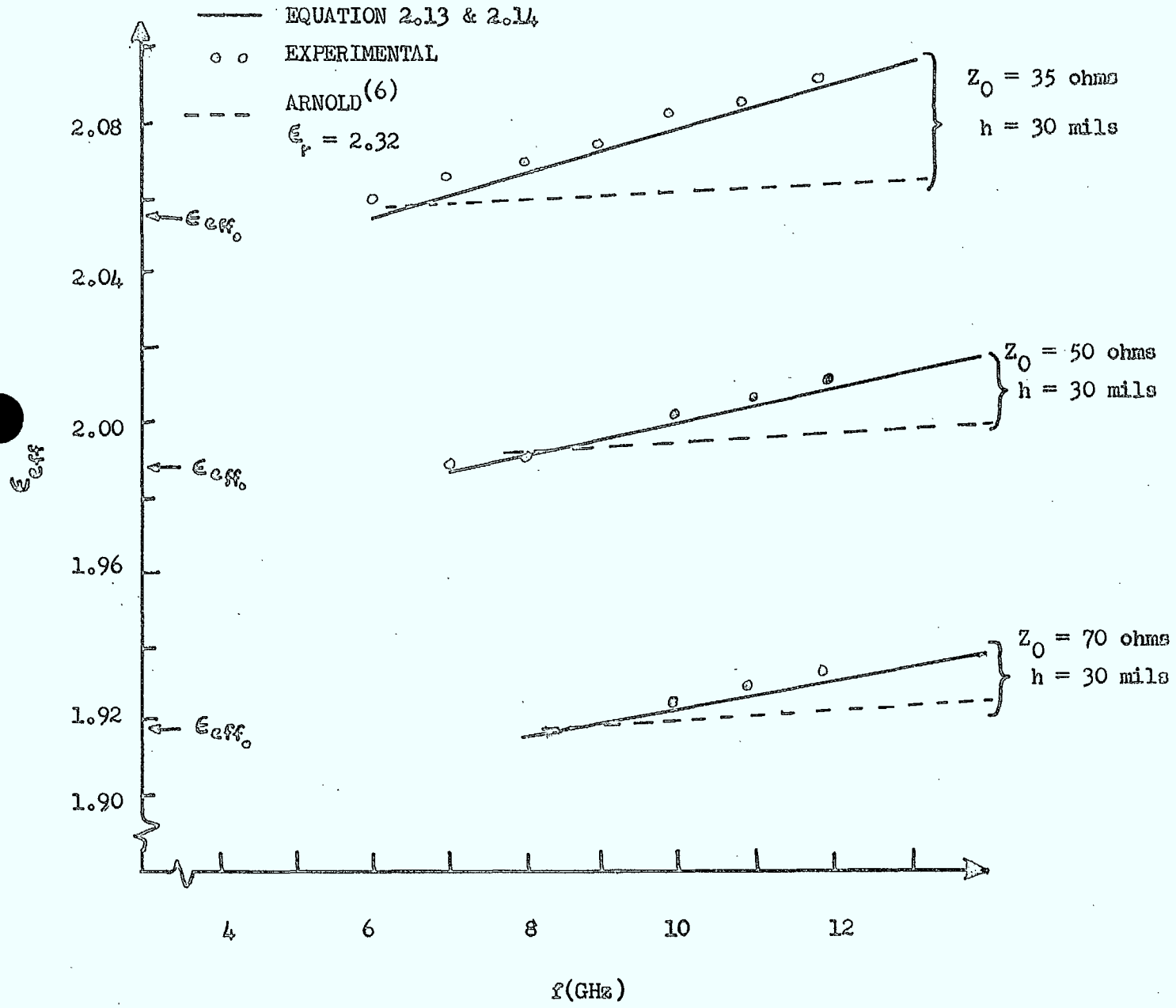

FIG. 12 EXPERIMENTAL AND EMPIRICAL RESULTS ON DISPERSION.

($\epsilon_r = 2.32$, h = 30 mils)

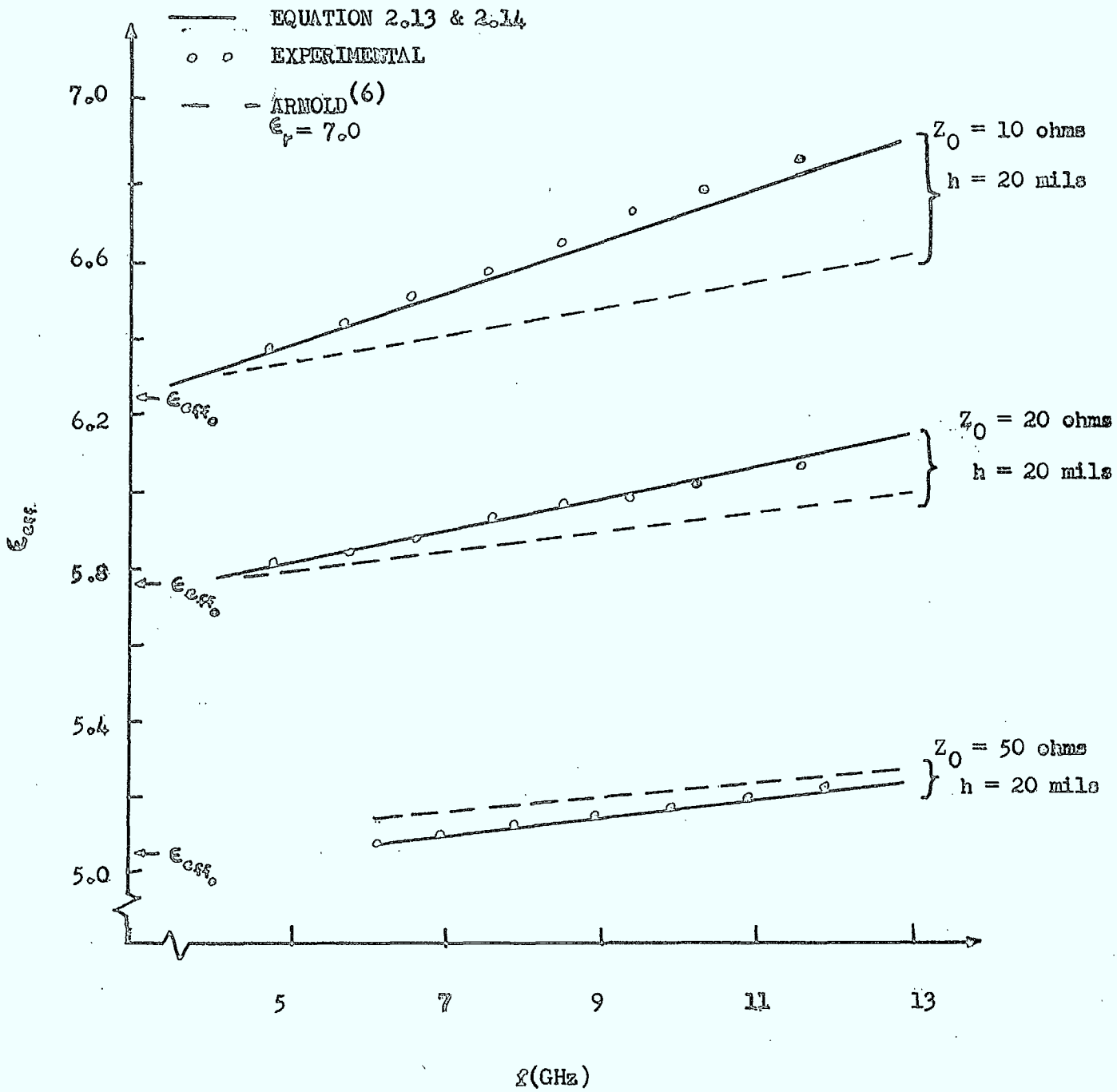

FIG. 13 EXPERIMENTAL AND EMPIRICAL RESULTS ON DISPERSION.

($\epsilon_r = 7.0$, h = 20 mils)

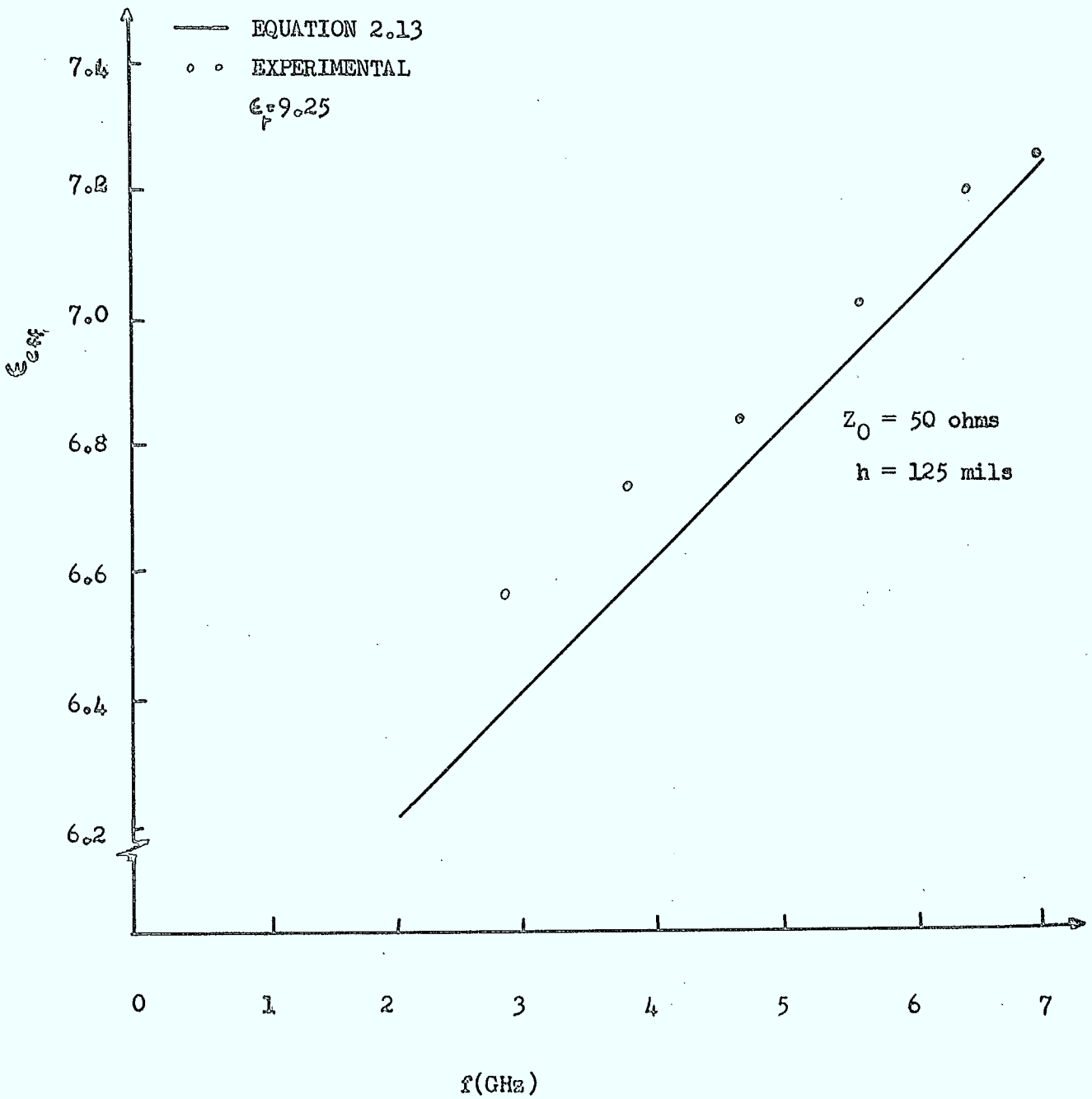

FIG. 14 EXPERIMENTAL AND EMPIRICAL RESULTS ON DISPERSION.

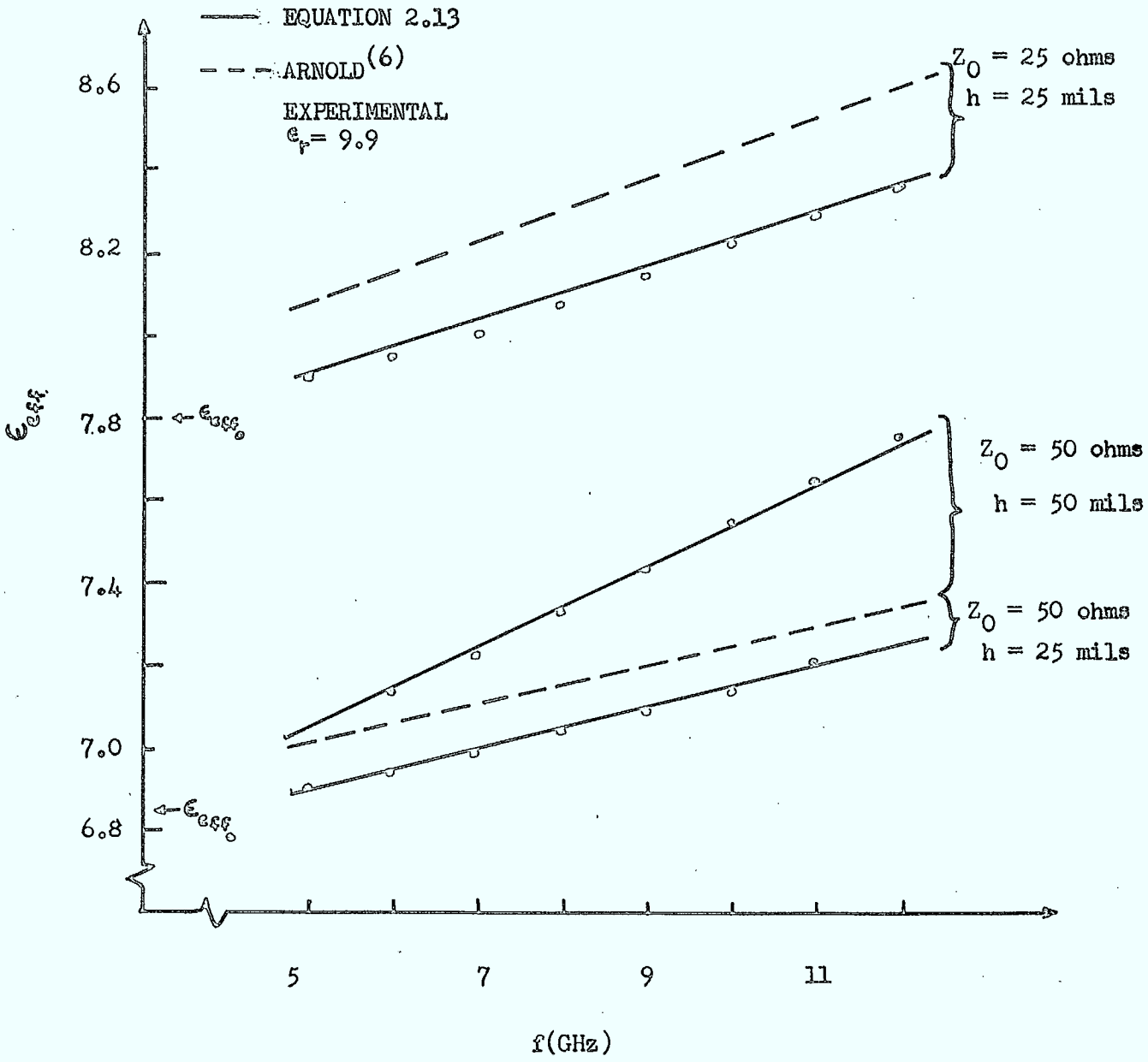

FIG. 15 EXPERIMENTAL AND EMPIRICAL RESULTS ON DISPERSION .

(ϵ_r = 9.9, h = 25 & 50 mils)

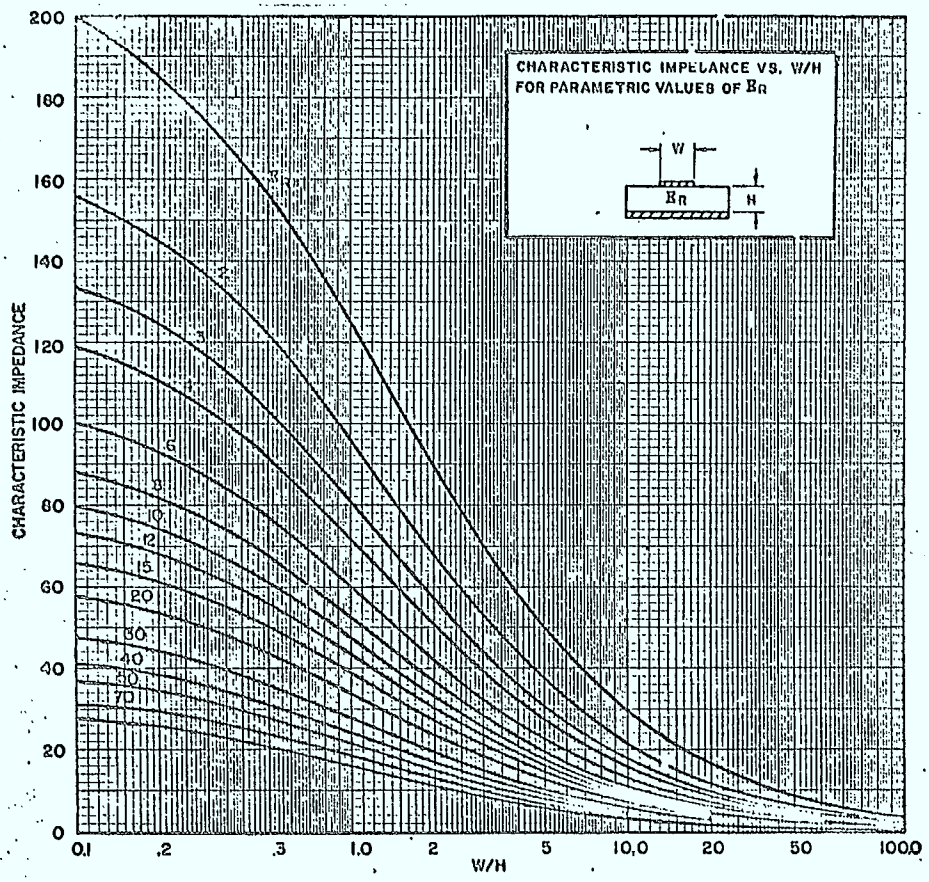

FIG. 16a CHARACTERISTIC IMPEDANCE VS. $\frac{W}{h}$ FOR PARAMETRIC VALUES OF ϵ_r (Wheeler's Curves). (33)

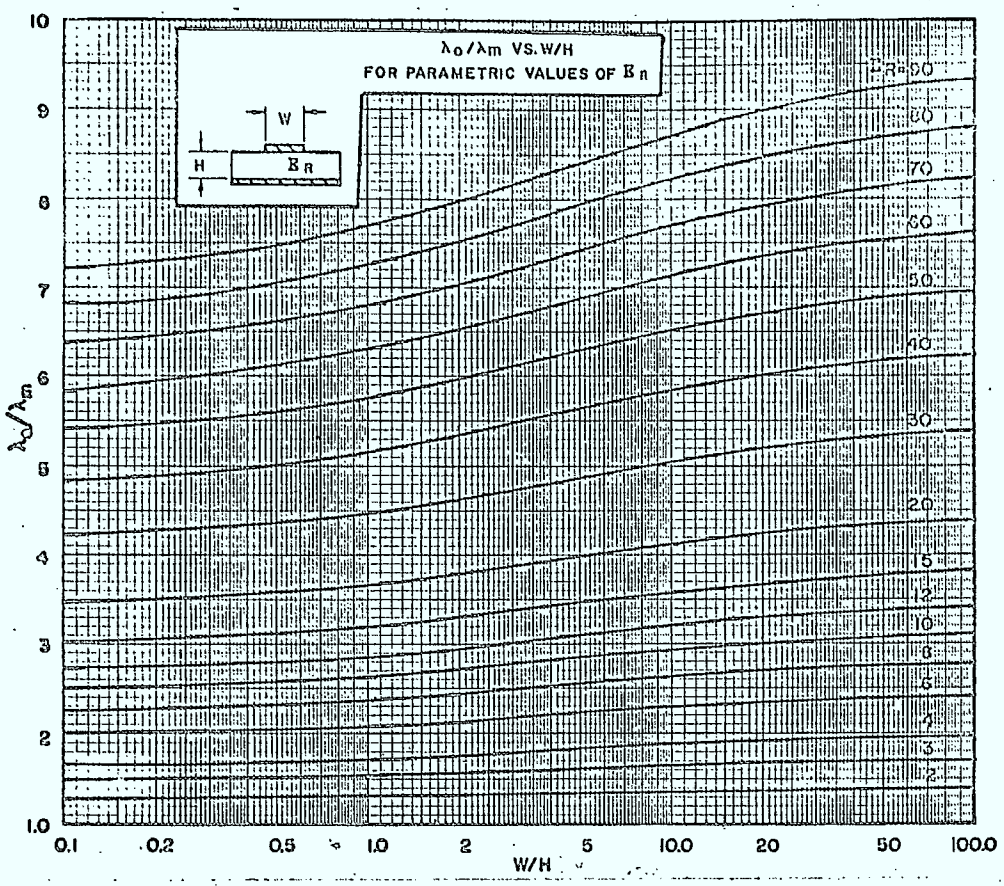

FIG. 16b $\frac{\lambda_o}{\lambda_m}$ VS. $\frac{W}{h}$ FOR PARAMETRIC VALUES OF ϵ_r (Wheeler's Curves). (33)

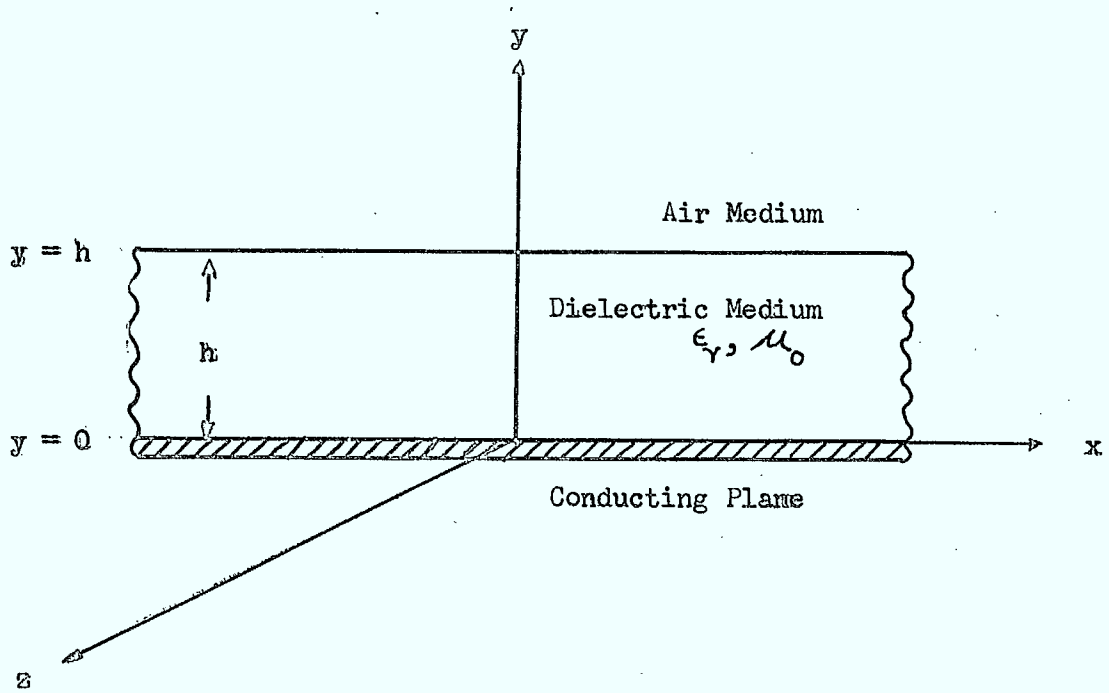

FIG. 17 DIELECTRIC SLAB ON A CONDUCTING PLANE.

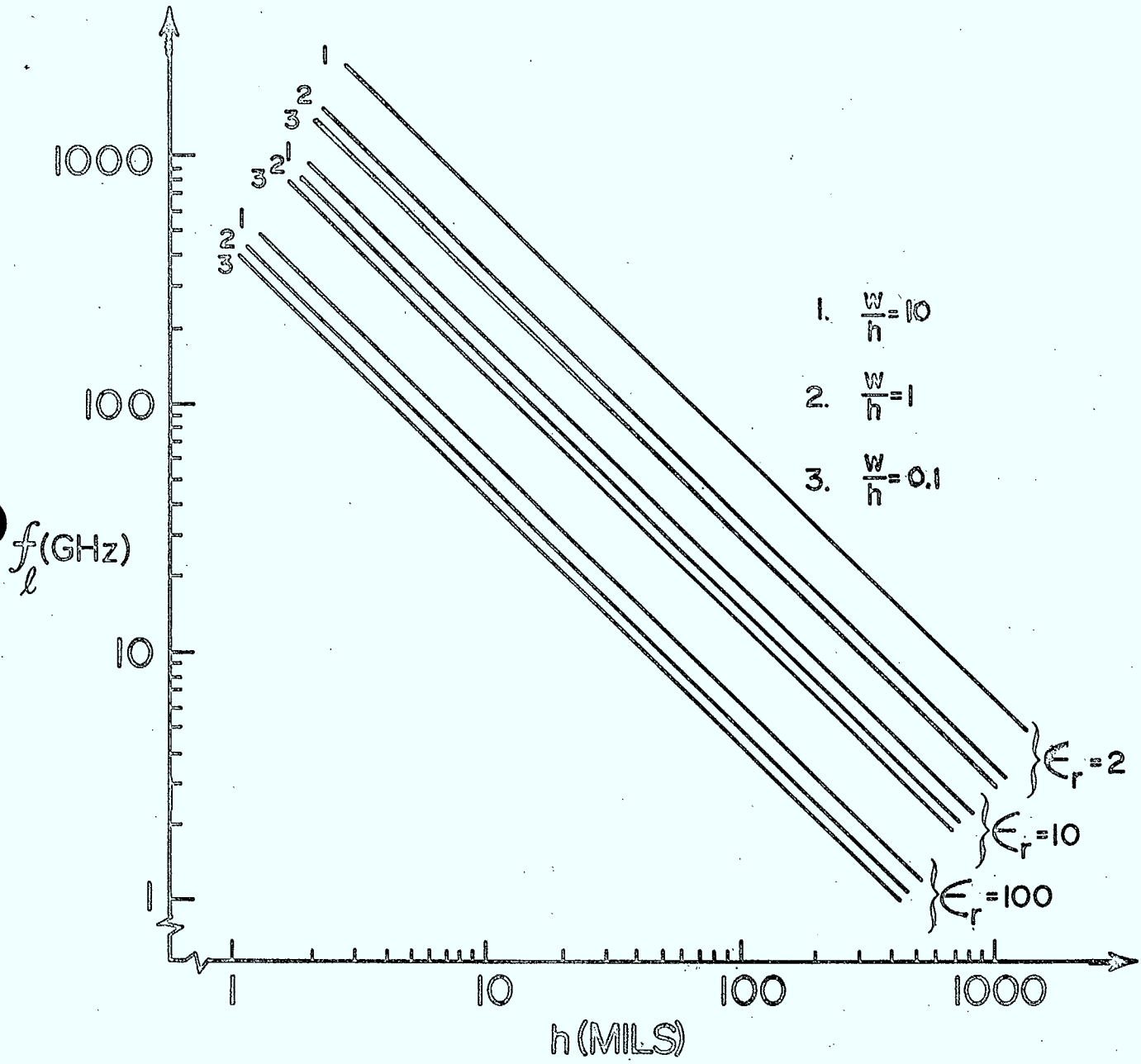

FIG. 18 UPPER FREQUENCY LIMIT VS. ϵ_r, h & w/h .

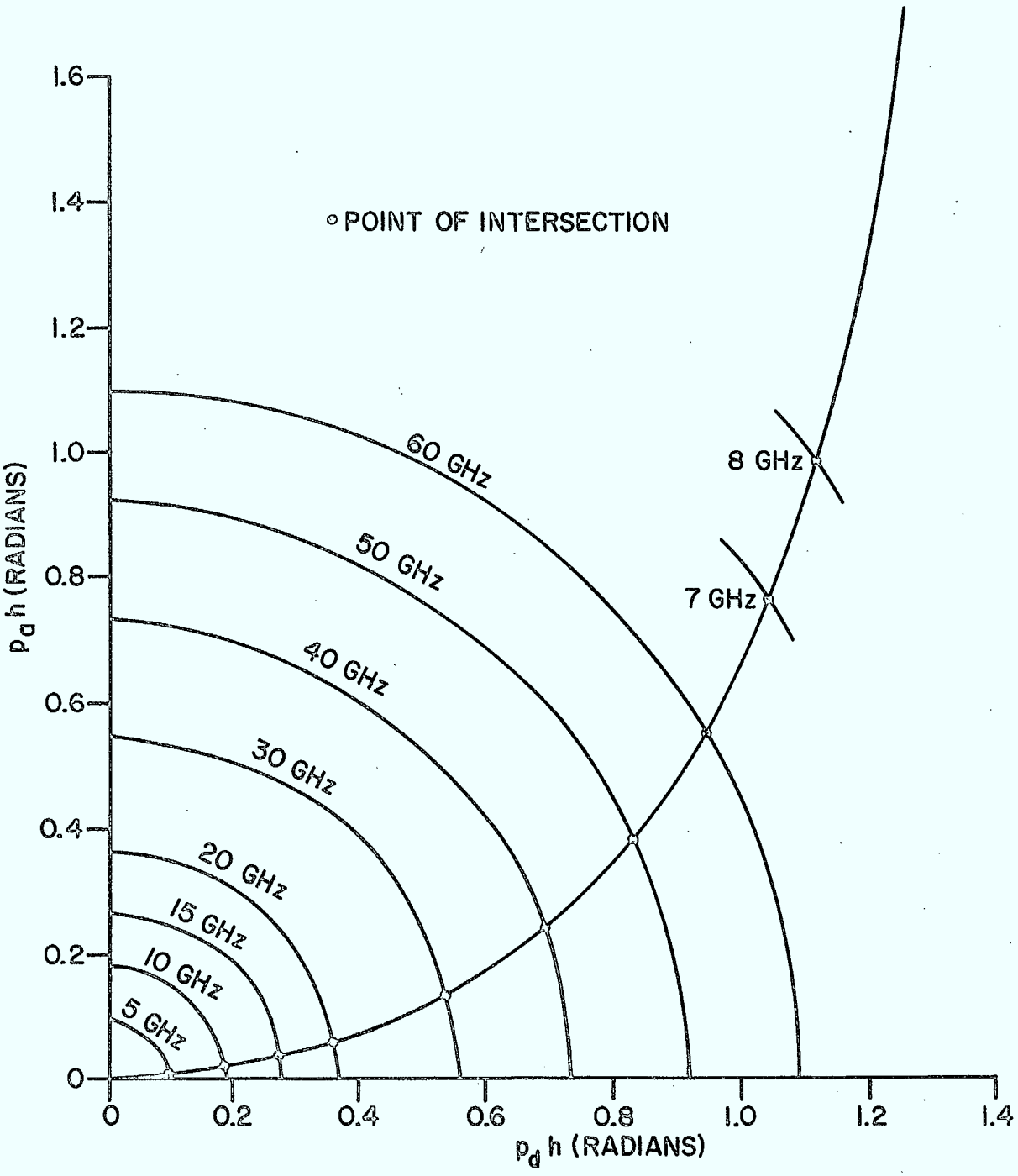

FIG. 19 - GRAPHICAL SOLUTION FOR THE TM_0 SURFACE WAVE MODE FOR $\epsilon_r = 2.32$, $h = 30$ MILS.

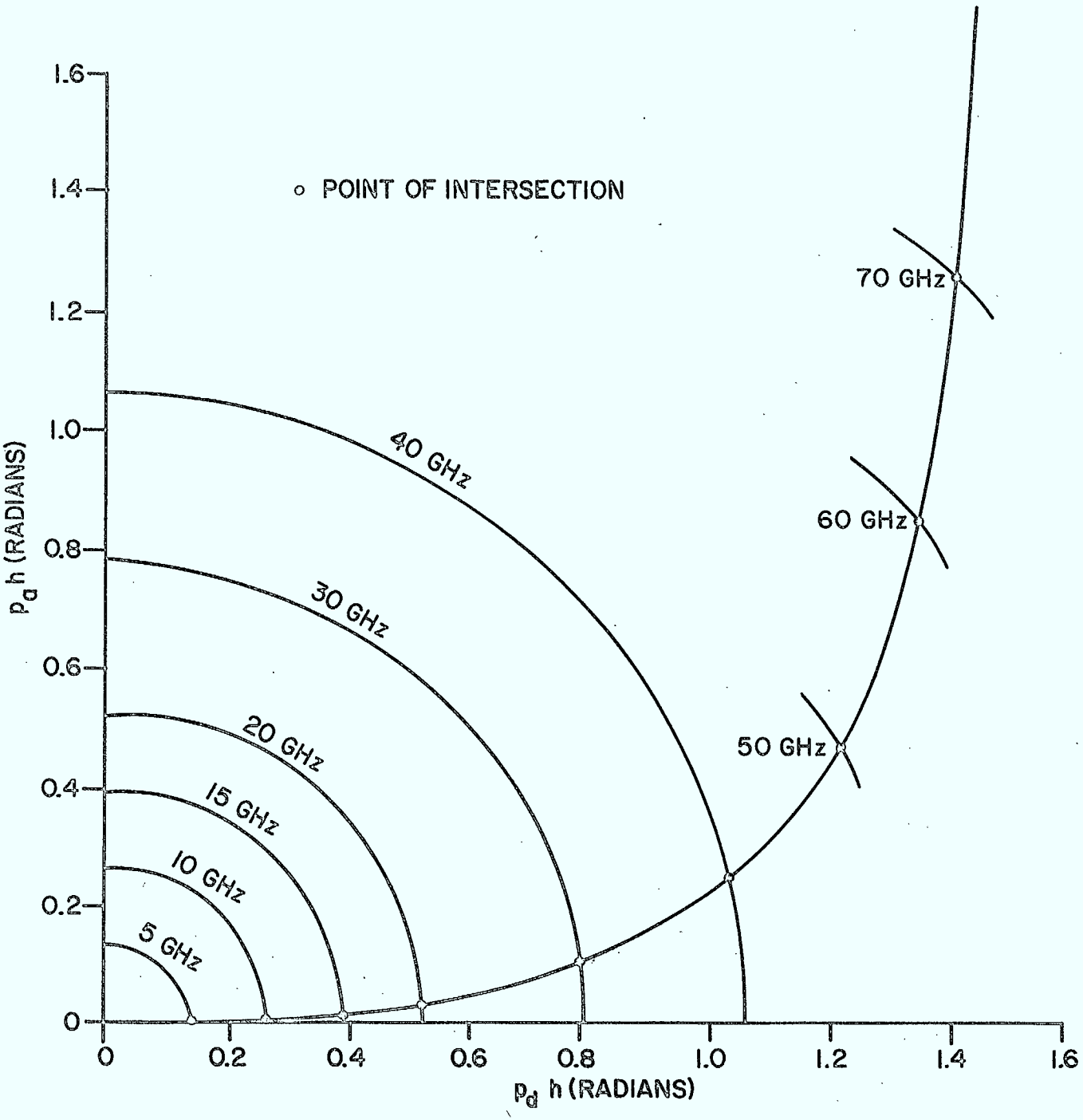

FIG. 20 – GRAPHICAL SOLUTION FOR THE TM_0 SURFACE WAVE MODE FOR $\epsilon_r = 7.0$, $h = 20$ MILS.

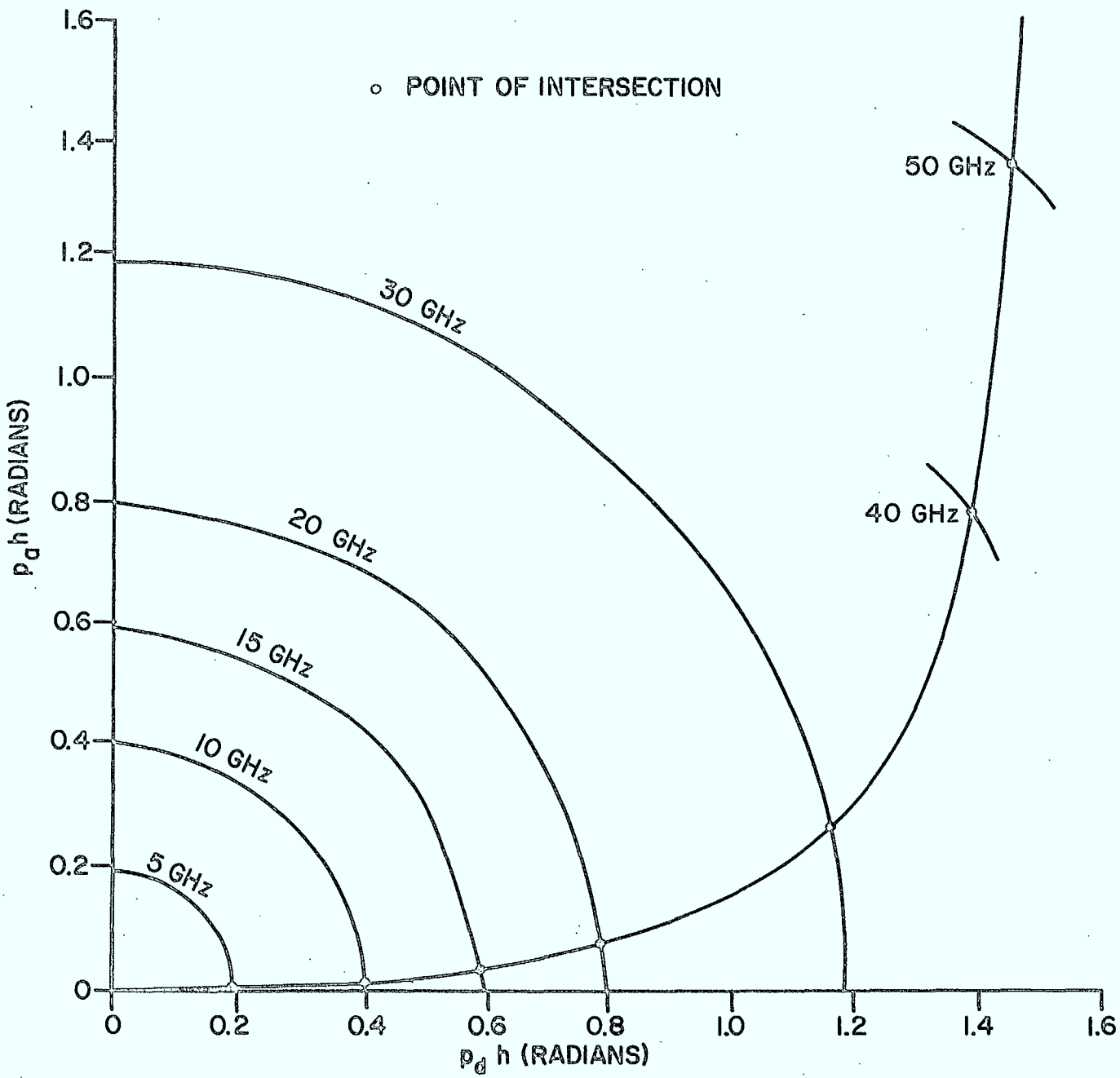

FIG. 21 – GRAPHICAL SOLUTION FOR THE TM_0 SURFACE WAVE MODE FOR $\epsilon_r = 9.9$, h = 25 MILS.

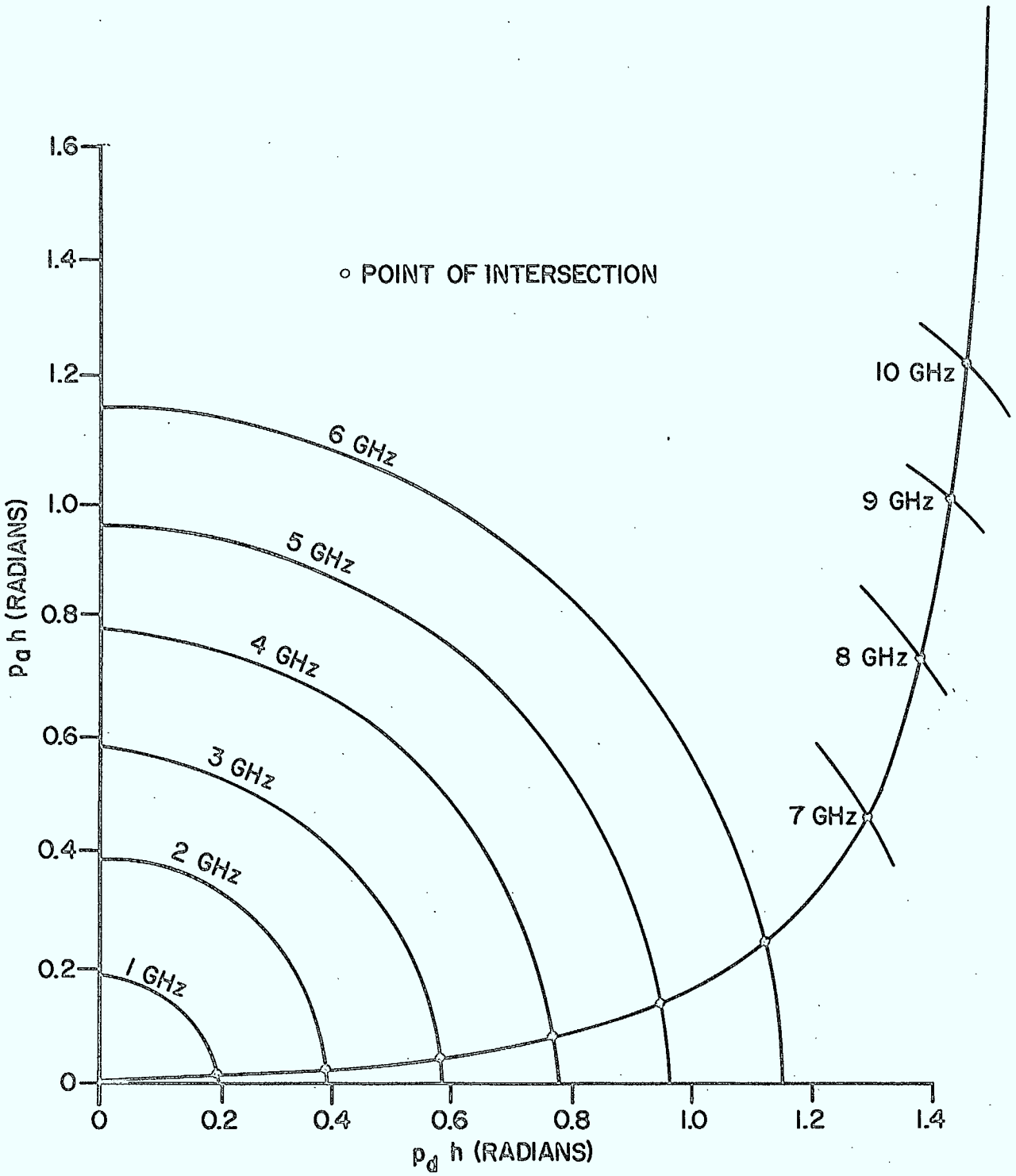

FIG. 22–GRAPHICAL SOLUTION FOR THE TM_0 SURFACE WAVE MODE FOR ϵ_r=9.25, h=125 MILS.

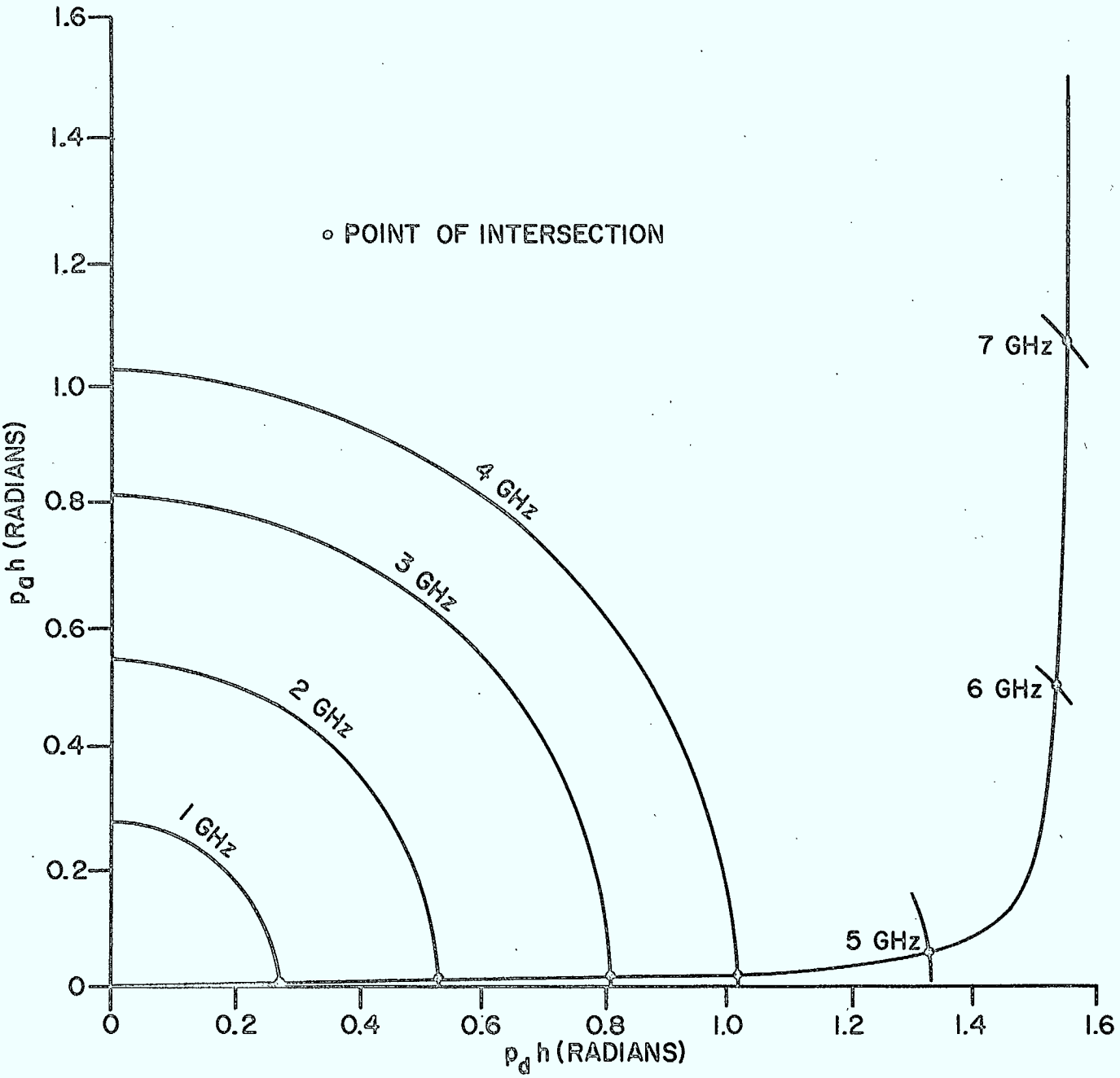

FIG. 23–GRAPHICAL SOLUTIONS FOR THE TM_0 SURFACE WAVE MODE FOR $\epsilon_r = 10.4$, h=50 MILS.

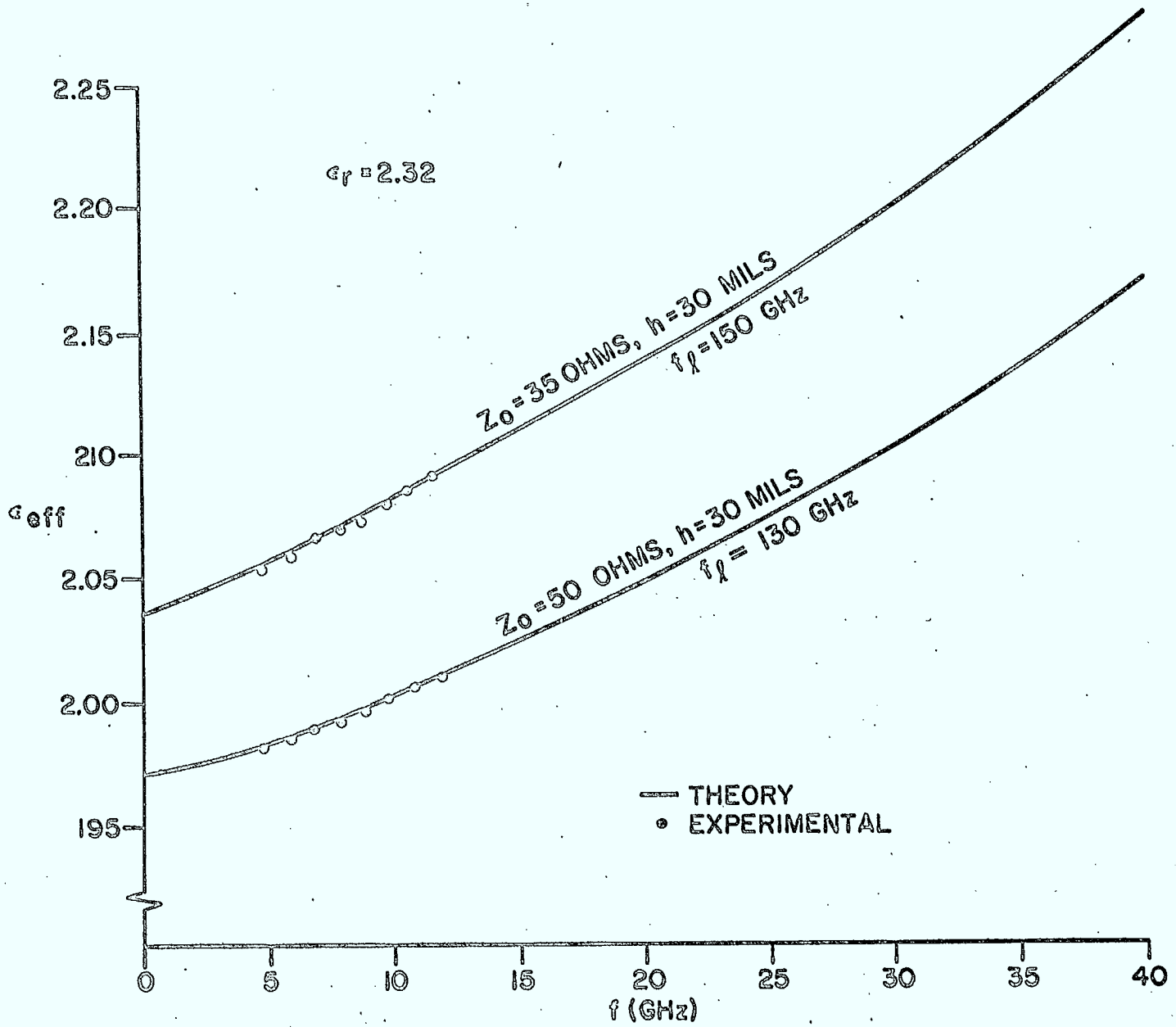

FIG. 24 EXPERIMENTAL AND ANALYTICAL RESULTS ON DISPERSION.
($\epsilon_r = 2.32$, h = 30 mils)

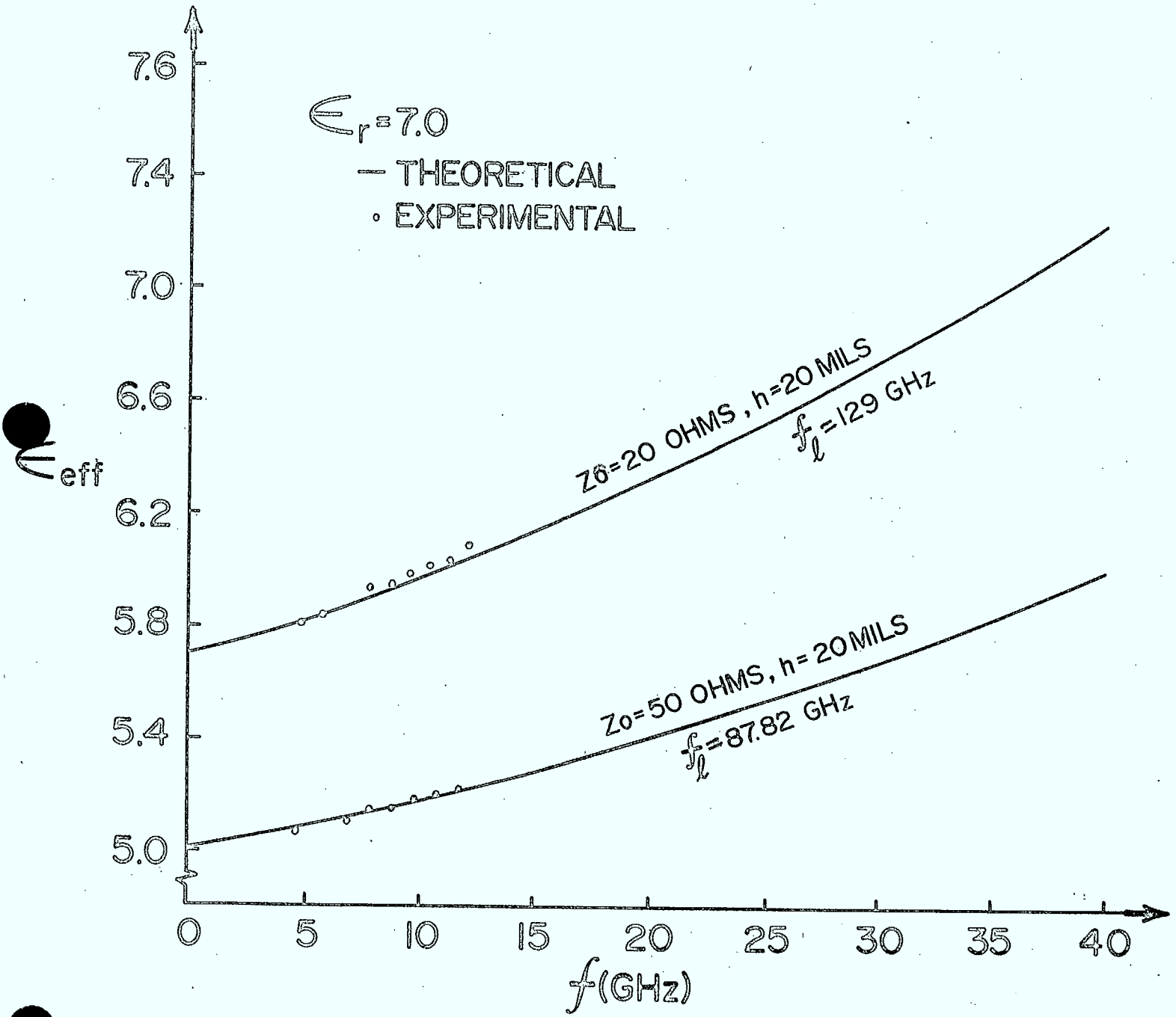

FIG. 25 EXPERIMENTAL AND ANALYTICAL RESULTS ON DISPERSION.
(ϵ_r = 7.0, h = 20 mils)

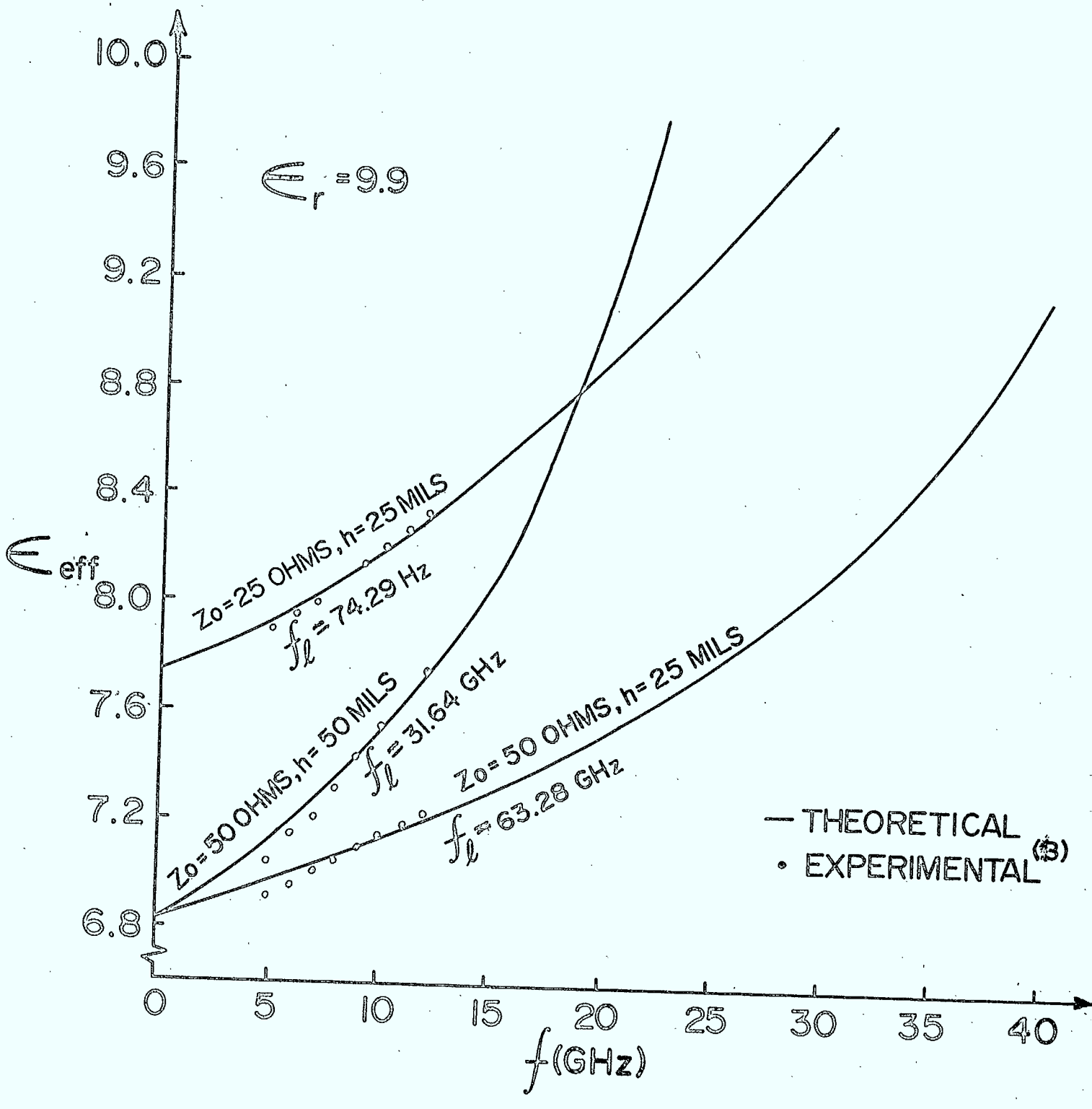

FIG. 26 EXPERIMENTAL AND ANALYTICAL RESULTS ON DISPERSION.
(ϵ_r = 9.9, h = 25 & 50 mils)

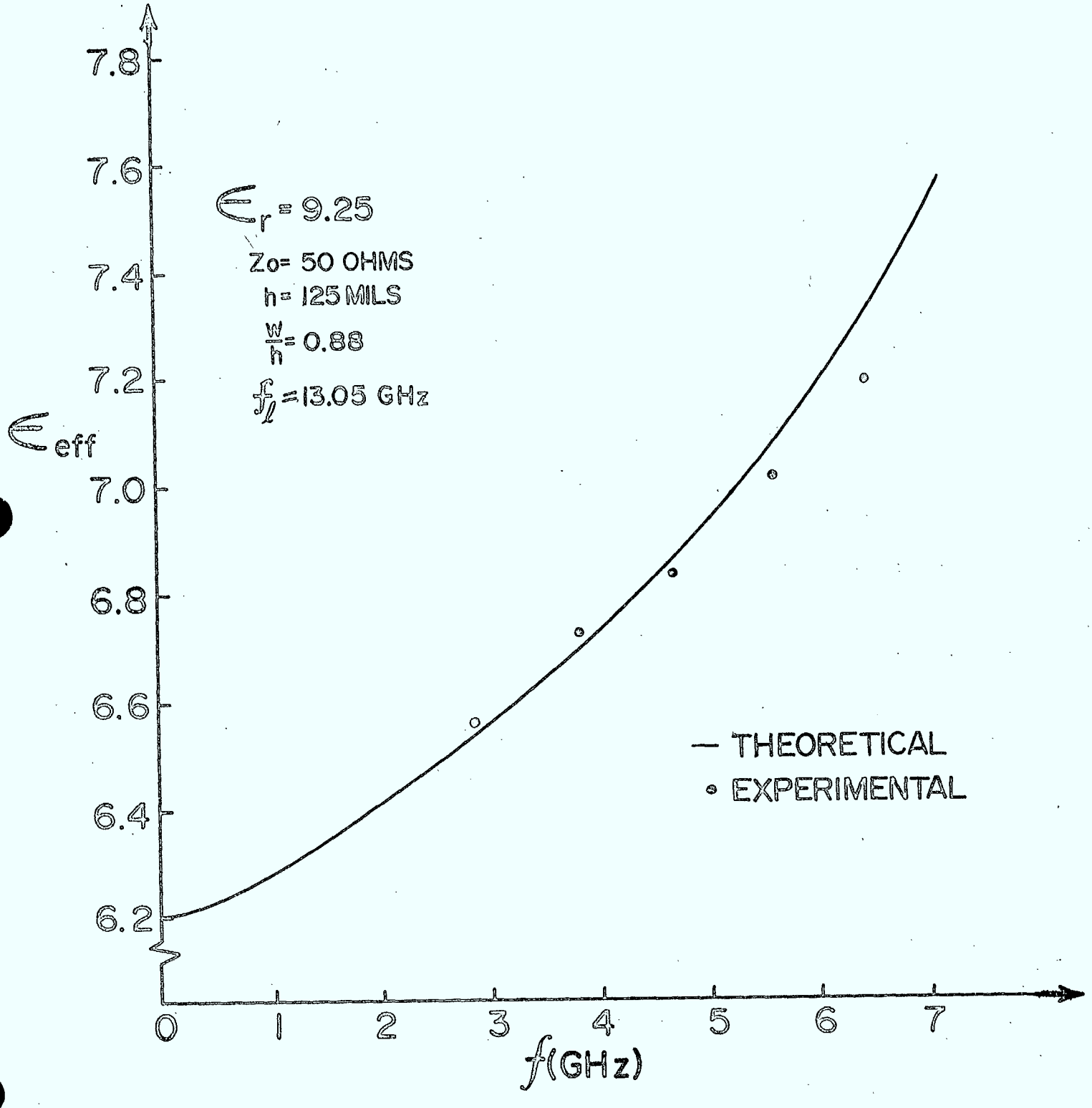

FIG. 27 EXPERIMENTAL AND ANALYTICAL RESULTS ON DISPERSION.
($\epsilon_r = 9.25$, h = 125 mils)

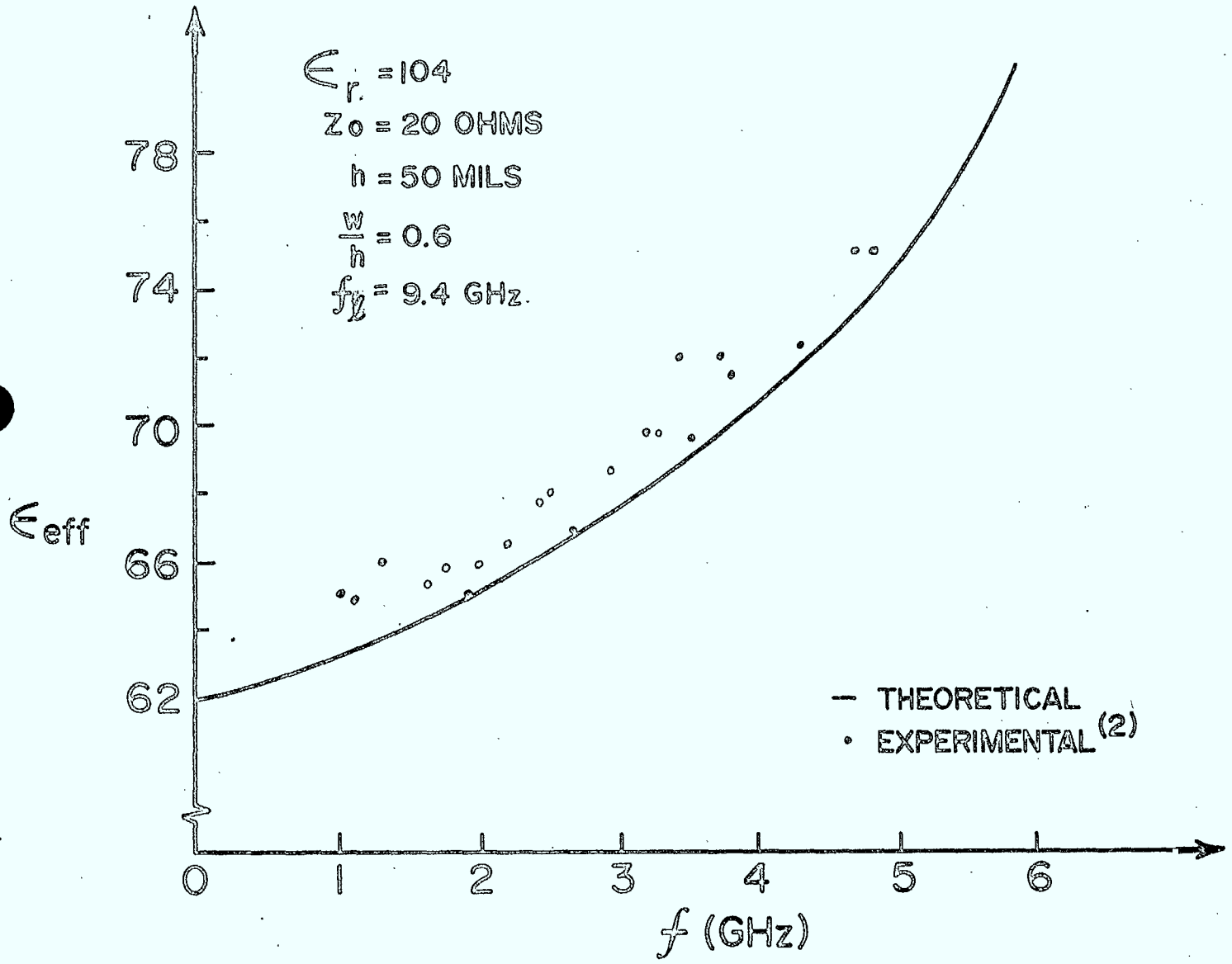

FIG. 28 EXPERIMENTAL AND ANALYTICAL RESULTS ON DISPERSION.
(ϵ_r = 104, h = 50 mils)

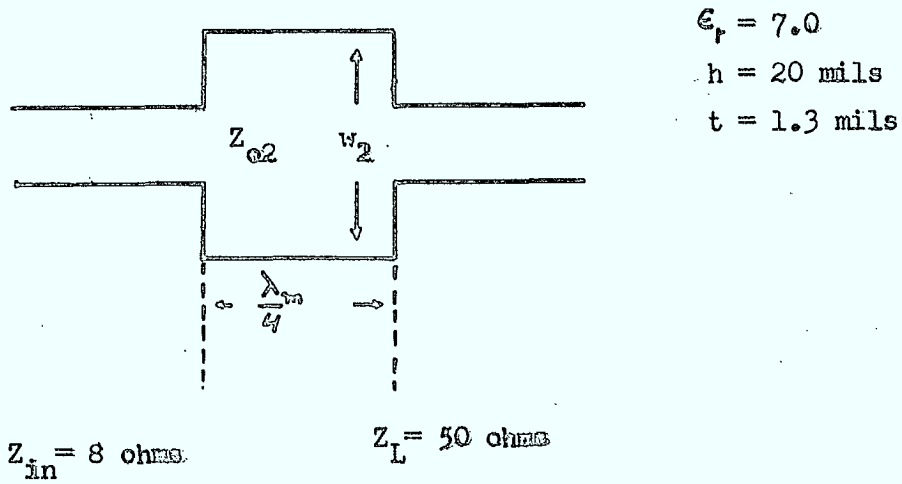

FIG. 29 A QUARTER WAVE TRANSFORMER FOR DESIGN EXAMPLE .

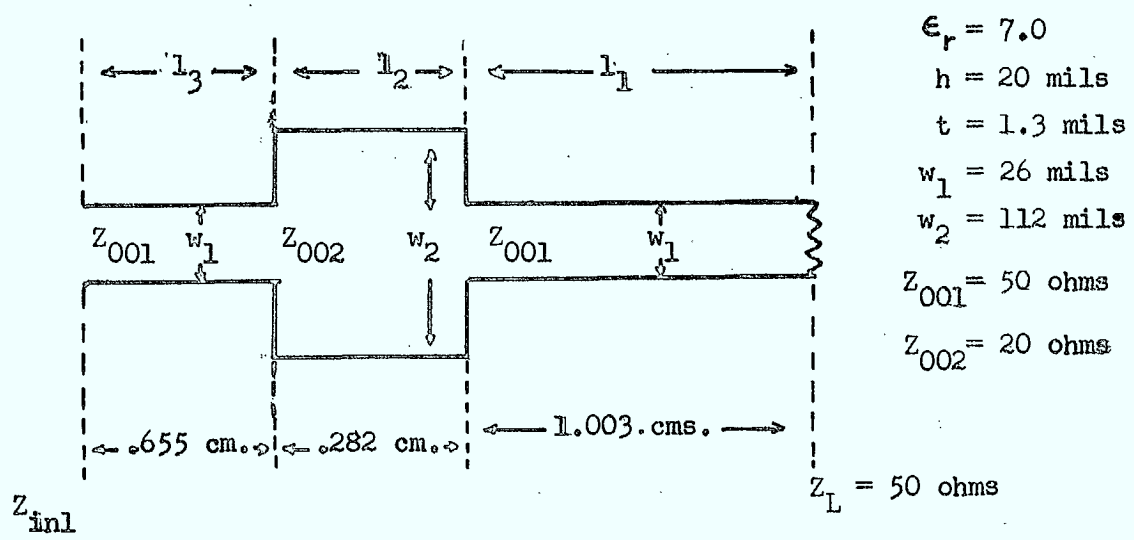

FIG. 30 A QUARTER WAVE TRANSFORMER FOR EXPERIMENTAL VERIFICATION.

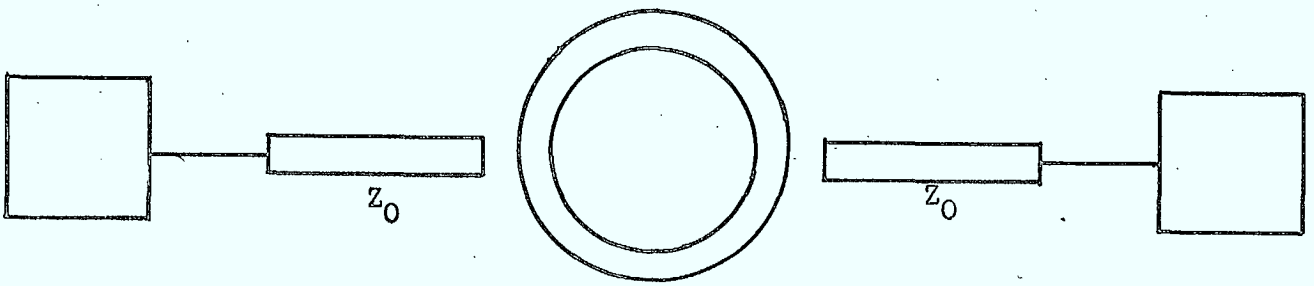

SIGNAL GENERATOR | MICROSTRIP TRANSMISSION LINE OF LENGTH l_1 | MICROSTRIP RESONANT CAVITY | MICROSTRIP TRANSMISSION LINE OF LENGTH l_2 | DETECTOR

(a)

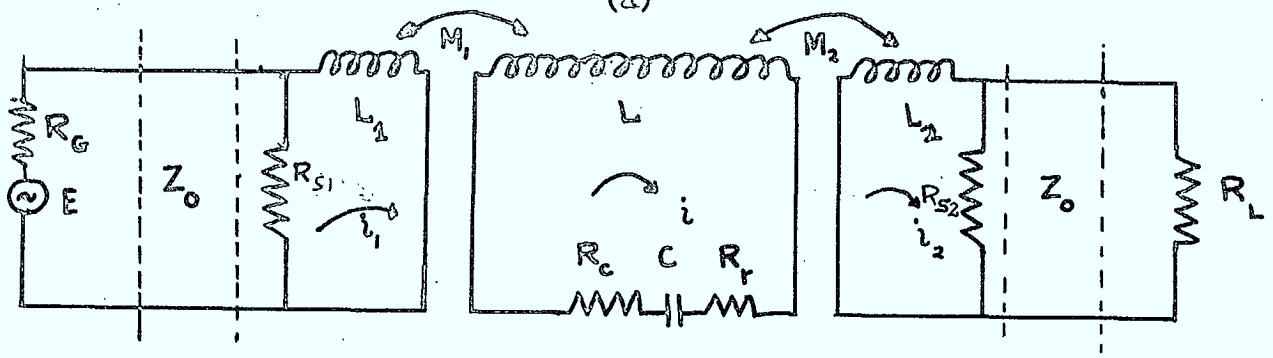

(b)

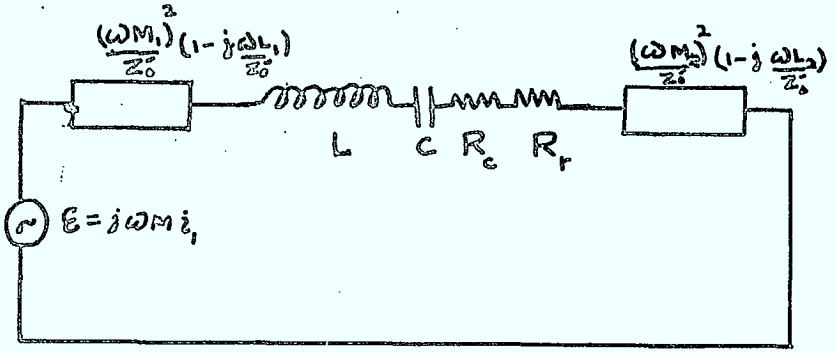

(c)

FIG. A.1a A MICROSTRIP RESONANT CAVITY CONNECTED BETWEEN A SIGNAL GENERATOR AND A DETECTOR.

FIG. A.1b THE EQUIVALENT CIRCUIT USING MUTUAL INDUCTANCES AS COUPLING ELEMENTS.

FIG. A.1c THE EQUIVALENT CIRCUIT REFERRED TO THE CAVITY ASSUMING $R_G = R_L = Z_0$, & $R_{s1} = R_{s2} = R_s$.

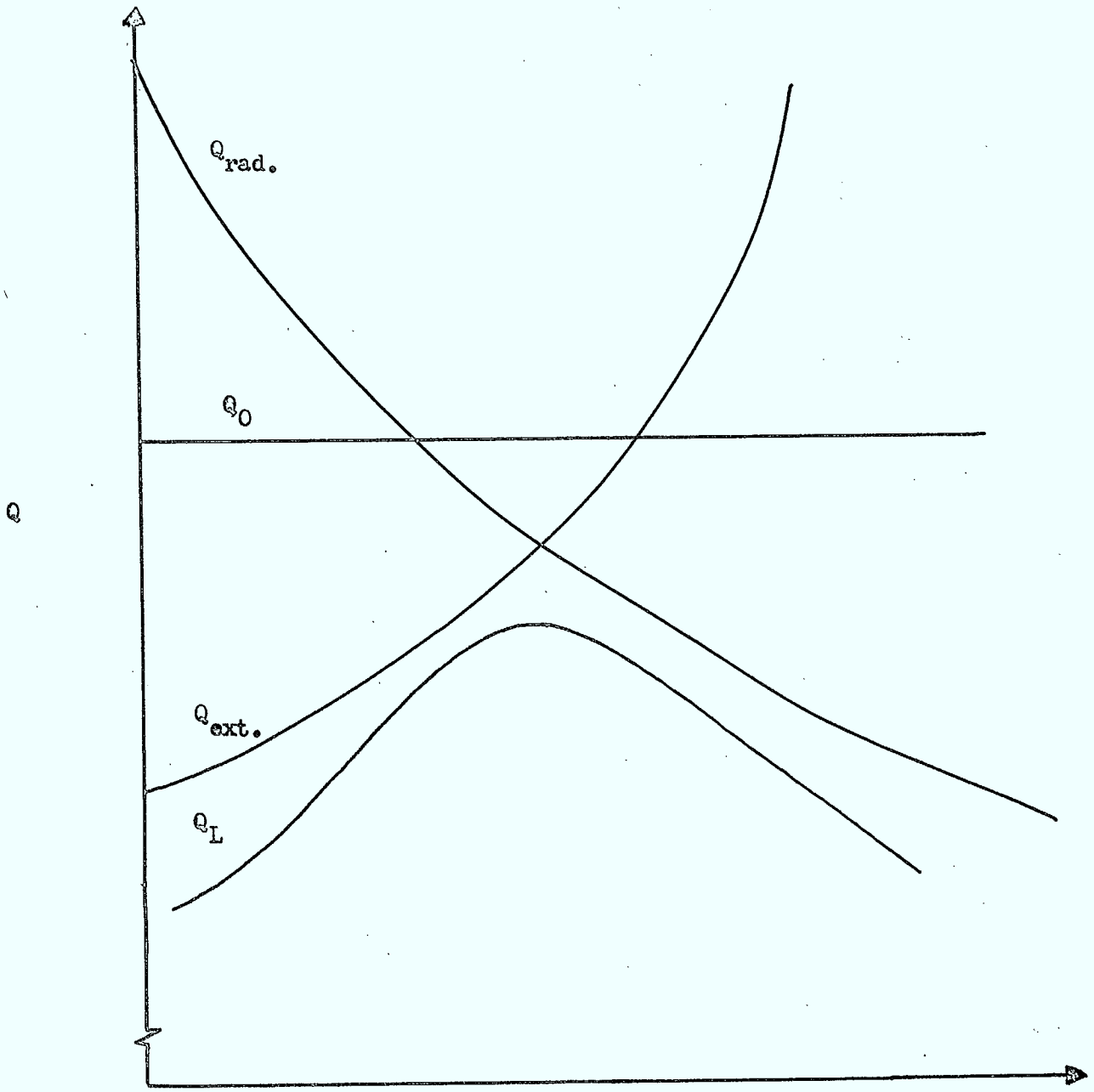

FIG. A.2 A TYPICAL VARIATION OF Q_0, $Q_{rad.}$, $Q_{ext.}$ & Q_L WITH COUPLING GAP.

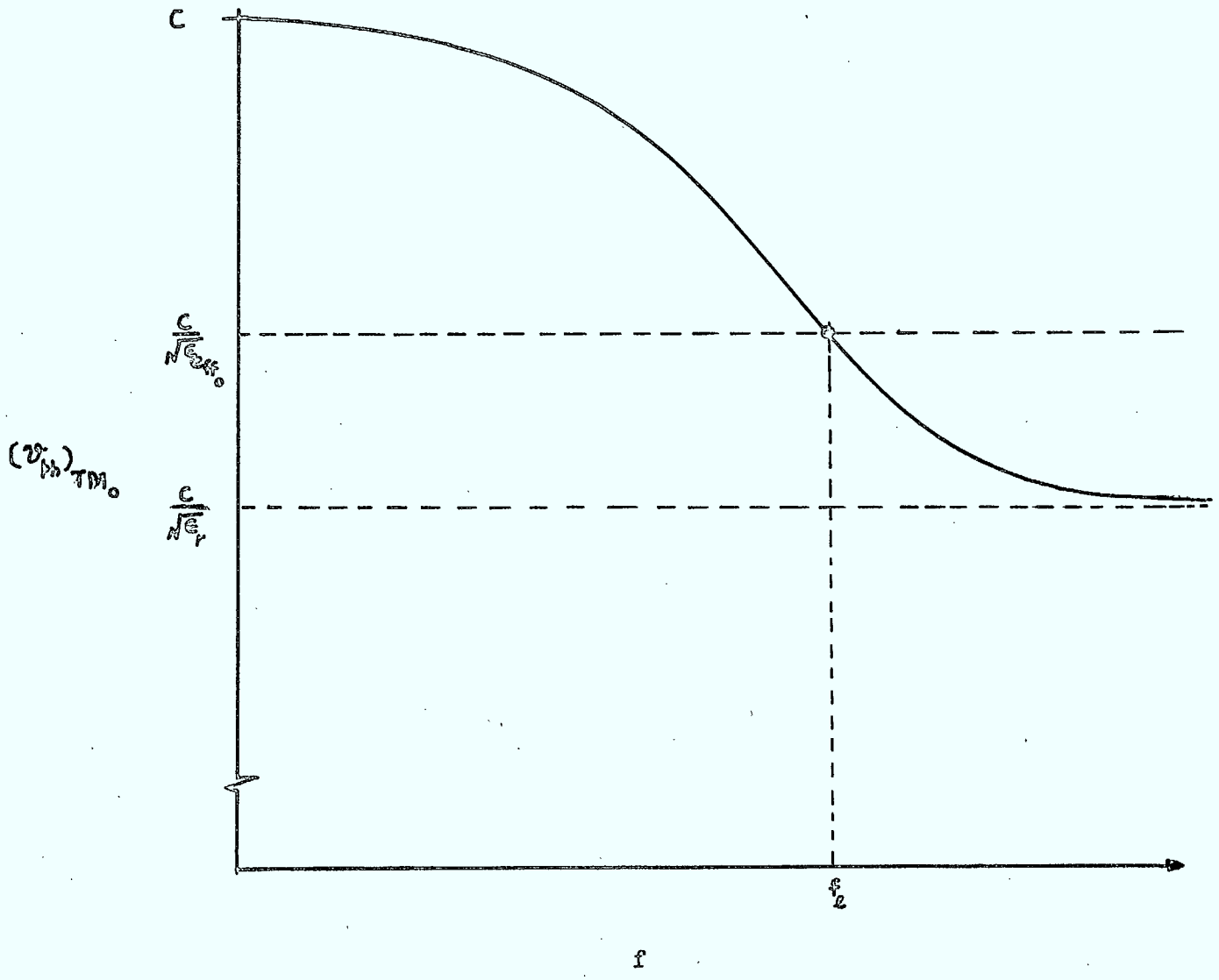

FIG. B.1 A TYPICAL VARIATION OF THE PHASE VELOCITY OF THE TM_0 SURFACE WAVE MODE VS. FREQUENCY.

BIBLIOGRAPHY

1. C.P. Hartwig, D. Masse and R.A. Pucel, *"Frequency Dependent Behaviour of Microstrip"*, G-MTT Interna'l Microwave Symp., Detroit, Michigan, pp 110-116, May 20-22, 1968.

2. P. Troughton, *"Measurement Techniques in Microstrips"*, Electronic Letters, Vol. 5, pp 25-26, January 23, 1969.

3. P. Troughton, *"The Evaluation of Alumina Substrate for Use in Microstrip Microwave Integrated Circuits"*, 1969 European Microwave Conference, IEE Conference Publication 58, pp 49-52, 1970.

4. G.I. Zysman and Varon, *"Wave Propagation in Microstrip Transmission Lines"*, G-MTT Interna'l Microwave Symp., Dallas, Texas, pp 3-9, May 5-7, 1969.

5. L.S. Napoli and J.J. Hughes, *"High Frequency Behaviour of Microstrip Transmission Lines"*, RCA Review, Vol. 30, pp 268-276, June 1969.

6. S. Arnold, *"Dispersive Effects in Microstrip on Alumina Substrate"*, Electronics Letters, Vol. 5, pp 673-674, December 1969.

7. G.K. Grunberger, V. Keine, H.H. Meinke, *"Longitudinal Field Components and Frequency Dependent Phase Velocity in the Microstrip Line"*, Electronic Letters, Vol. 6, pp 683-685, October 15, 1970.

8. J.B. Davis and D.G. Con, *"Computer Analysis of the Fundamental and Higher Order Modes in Single and Coupled Microstrip"*, Electronic Letters, Vol. 6, pp 806-808, December 10, 1970.

9. M. Arditi, *"Characteristics and Application of Microstrip for Microwave Wiring"*, IRE Trans., Microwave Theory and Techniques, Vol. MTT-3, pp 31-56, March 1955.

10. M.V. Schneider, *"Microstrip Lines for Microwave Integrated Circuits"*, The Bell System Technical Journal, pp 1421-1443, May - June 1969.

BIBLIOGRAPHY (Cont'd)

11. L. Lewin, *Radiation from Discontinuties in Strip Line"*, Proc. IEE (London), Vol. 107, Pt. C, pp 163-170, Feb. 1960.

12. E.J. Denlinger, *"Radiation from Microstrip Resonators"*, IEEE Trans., Microwave Theory and Techniques (Correspondence), Vol. MTT-17, pp 235-236, April 1969.

13. M.A.R. Gunsten and J.R. Weale, *"The Transmission Line Characteristics of Microstrip"*, The Marconi Review, Third Quarter, pp 226-243, 1969.

14. H.A. Wheeler, *"Transmission Line Properties of Parallel Strips Separated by a Dielectric Sheet"*, IEEE Trans., Microwave Theory and Techniques, Vol. MTT-13, pp 172-185, March 1965.

15. H.E. Steinhelfer, *"An Accurate Calculation of Uniform Microstrip Lines"*, IEEE Trans., Microwave Theory and Techniques, Vol. MTT-16, pp 439-444, July 1968.

16. E. Yamashita and R. Mitra, *"Variational Method for the Analysis of Microstrip Lines"*, IEEE Trans., Microwave Theory and Techniques, Vol. MTT-16, pp 251-256- April 1968.

17. M. Caulton, J.J. Hughes and H. Sobol, *"Measurement on the Properties of Microstrip Transmission Lines for Microwave Integrated Circuits"*, RCA Review, Vol. 27, pp 377-391, September 1966.

18. T.T. Wu, *"Theory of Microstrip"*, Journal of Applied Physics, Vol. 28, No. 5, pp 299-302, March 1957.

19. P. Delogne, *"On Wu's Theory of Microstrip"*, Electronics Letters, Vol. 6, No. 17, August 20, 1970.

20. G.D. Vendelin, *"Limitations on Microstrip Line Q"*, Microwave Journal, Vol. 13, No. 5, pp 63-69, May 1970.

21. M. Arditi, *"Experimental Determination of the Properties of Microstrip Components"*, Electrical Communications, Vol. 30, pp 283-293, December 1953.

22. E.L. Ginzton, *"Microwave Measurements"*, New York: McGraw-Hill, 1957, pp 226-234.

23. C.P. Hartwig, *"Basic Parameters of Microstrip Transmission Lines"*, IEEE International Convention, 1970.

24. E.L. Ginzton, *"Microwave Measurements"*, New York: McGraw-Hill, 1957, pp 349-355, 391-405.

25. M. Sucher and J. Fox, *"Handbook of Microwave Measurements"*, New York: Polytechnic Press of Polytechnic Institute of Booklyn, 1963, Third Edition, Vol. 2, pp 417-491.

BIBLIOGRAPHY (Cont'd)

26. R.A. Pucel, D.J. Masse and C.P. Hartwig, *"Losses in Microstrip"*, IEEE Trans., Microwave Theory and Techniques, Vol. MTT-16, pp 342-350, June 1968.

27. C.G. Shafer, *"Higher Mode of the Microstrip Transmission Line"*, Cruft Lab., Harvard University, Cambridge, Mass., Tech. Rept. 258, Nov. 25, 1957.

28. R.E. Collin, *"Foundations for Microwave Engineering"*, New York: McGraw-Hill, 1966, pp 113-117.

29. C.C. Johnson, *"Field and Wave Electrodynamics"*, New York: McGraw-Hill, 1965, pp 296-299.

30. R.E. Collin, *"Field Theory of Guided Waves"*, New York: McGraw-Hill, 1960, pp 453-474.

31. W.J. Chudobiak, O.P. Jain and V. Makios, *"Dispersion in Microstrip"*, to be published, IEEE Trans. Microwave Theory and Techniques.

32. O.P. Jain, V. Makios and W.J. Chudobiak, *"The Dispersive Behaviour of Microstrip Transmission Lines"*, to be published in the proceedings of 1971 European Microwave Conference, Stockholm, Sweden, August 1971.

33. The Microwave Engineer's Handbook and Buyer's Guide, Brookline, Mass: Horizon House - Microwave, Inc., 1969, pp 65-66.